Symbiosis at its limits: ecophysiological consequences of lichenization to the genus Prasiola in Antarctica

Symbiosis at its limits: ecophysiological consequences of lichenization to the genus *Prasiola* in Antarctica

Beatriz Fernández-Marín[1,8*], Marina López-Pozo[1], Alicia V. Perera-Castro[2], Miren Irati Arzac[1], Ana Saenz-Ceniceros[1], Claudia Colesie[3], Asunción de los Ríos[4], Leo G. Sancho[5], Ana Pintado[5], José M. Laza[6], Sergio Pérez-Ortega[7], José I. García-Plazaola[1]

[1] Department of Plant Biology and Ecology. University of the Basque Country (UPV/EHU). Barrio Sarriena sn, 48940 Leioa, Spain; [2] Research Group on Plant Biology under Mediterranean Conditions, Universitat de les Illes Balears (UIB) - Instituto de Investigaciones Agroambientales y de Economía del Agua (INAGEA), Carretera de Valldemossa Km 7.5, 07122, Palma, Illes Balears, Spain; [3] Global Change Institute, School of GeoSciences, University of Edinburgh, Alexander Crum Brown Road, Edinburgh EH9 3FF, UK; [4] Museo Nacional de Ciencias Naturales (MNCN-CSIC), Serrano 115 dpdo, 28006 Madrid, Spain; [5] Dept Biol Vegetal 2, Fac Farm. Universidad Complutense, 28040 Madrid, Spain; [6] Laboratory of Macromolecular Chemistry (Labquimac). Department of Physical Chemistry. University of the Basque Country (UPV/EHU). Barrio Sarriena sn, 48940 Leioa, Spain; [7] Real Jardín Botánico (RJB-CSIC), Plaza de Murillo 2, 28014 Madrid, Spain; [8] Department of Botany, Ecology and Physiology. University of La Laguna (ULL), 38200 La Laguna, Canarias, Spain

For correspondence. E-mail beatriz.fernandezm@ehu.es

- **Background and Aims** Lichens represent a symbiotic relationship between at least one fungal and one photosynthetic partner. The association between the lichen-forming fungus *Mastodia tessellata* (Verrucariaceae) and different species of *Prasiola* (Trebouxiophyceae) has an amphipolar distribution and represents a unique case study for the understanding of lichen symbiosis because of the macroalgal nature of the photobiont, the flexibility of the symbiotic interaction and the co-existence of free-living and lichenized forms in the same microenvironment. In this context, we aimed to (1) characterise the photosynthetic performance of co-occurring populations of free-living and lichenized *Prasiola* and (2) assess the effect of the symbiosis on the water relations in *Prasiola*, including its tolerance to desiccation and its survival and performance under sub-zero temperatures.
- **Methods** Photochemical responses to irradiance, desiccation, and freezing temperature and pressure-volume curves of co-existing free-living and lichenized *Prasiola* thalli were measured *in situ* in Livingston Island (Maritime Antarctica). Analyses of photosynthetic pigment, glass transition and ice nucleation temperatures, surface hydrophobicity extent and molecular analyses were conducted in the lab.
- **Key Results** Free-living and lichenized forms of *Prasiola* were identified as two different species: *P. crispa* and *Prasiola* sp., respectively. While the lichenization appears to have no effect on the photochemical performance of the alga, or in its tolerance to desiccation (at short-term), the symbiotic lifestyle involves (1) changes in water relations, (2) a considerable decrease in the net carbon balance and (3) an enhanced freezing tolerance.

- **Conclusions** Our results support an improved tolerance to subzero temperature as main benefit of lichenization for the photobiont, but highlight that lichenization represents a delicate equilibrium between a mutualistic and a less reciprocal relationship. In a warmer climate scenario, the spread of the free-living *Prasiola* in detriment of the lichen form would be likely, with unknown consequences for the Maritime Antarctic ecosystems.

Key words: abiotic stress, alga, desiccation tolerance, freezing tolerance, glassy state, lichen, *Mastodia tessellata*, photobiont, photoprotection, photosynthesis, polar, *Turgidosculum.*

INTRODUCTION

Lichens are symbiotic organisms resulting from the association of one fungal and, at least, one photosynthetic partner (mycobiont and photobiont, respectively). They can thrive in some of the harshest environments on Earth, such as drylands and tundra (e.g. Antarctica). As an illustrative example of their relevance, current Antarctic flora includes more than 350 species of lichens, around 130 species of bryophytes (100-115 mosses, and 27 liverworts) and only 2 species of tracheophytes (Kappen, 2000; Øvstedal & Lewis Smith, 2001; Peat *et al.*, 2007; Ochyra *et al.*, 2008). Lichens play essential roles in primary production and nutrient cycling in diverse ecosystems (Asplund & Wardle, 2017) including polar regions, where they represent a large fraction of the local biodiversity. Hence, the understanding of lichen ecophysiology as primary producers is of crucial relevance. With regard to climate change scenarios lichens receive increasing attention with particular emphasis on more vulnerable environments such as drylands and polar habitats (Laguna-Defior *et al.*, 2016; Bao *et al.*, 2018; Colesie *et al.*, 2018; Ladrón de Guevara *et al.*, 2018). In that sense, different manipulative experiments have recently indicated that: (i) increasing temperatures may alter lichen communities in drylands (Ladrón de Guevara *et al.*, 2018) and in the Antarctic (Colesie *et al.*, 2018), (ii) higher frequency of freezing/thawing events during winter may have negative impact on Arctic and Antarctic lichens (Harańczyk *et al.*, 2003; Bjerke, 2011) and (iii) prolonged period under snow may threat lichen subsistence in Maritime Antarctica (Bokhorst *et al.*, 2016; Sancho *et al.*, 2017).

Lichens are poikilohydric organisms and, the vast majority of the species are considered to be tolerant to desiccation, i.e. able to withstand extremely low cellular water contents (<0.1g H_2O g^{-1} DW) and to reactivate metabolic activity upon rehydration (Kranner *et al.*, 2008). In that sense, very finely tuned physiological and biochemical

processes, related mainly to photochemical and antioxidant protection, seem to be key aspects of their capacity to deal with severe cell dehydration (Kranner, 2002; Heber *et al.*, 2007; Fernández-Marín *et al.*, 2010). In dry lichens, a particular quenching of chlorophyll (Chl) fluorescence relates to the efficient dissipation of light energy during the dry periods (Veerman *et al.*, 2007; Heber *et al.*, 2010). Among antioxidants, zeaxanthin and glutathione seem to play a major role in the preservation of chloroplast and cell functionality during desiccation/rehydration cycles (Kranner *et al.*, 2003; Fernández-Marín *et al.*, 2010). Only recently, the loss of cell turgor has been pointed out as a relevant sensor and as trigger of desiccation-tolerance responses (Banchi *et al.*, 2018) and the physiology of their water relations is just starting to be addressed from irreversible thermodynamics approach, e.g. by measuring water potential isotherms (Nardini *et al.*, 2013; Petruzzellis *et al.*, 2018). Other physiochemical consequences of desiccation such as the entering in the so-called glassy state which severely limits biochemical reactions in desiccation-tolerant mosses and tracheophytes (Fernández-Marín *et al.*, 2013, 2018b), remains unexplored in lichens, so far.

Albeit lichens dominate cold environments and despite desiccation and low temperatures lead to many similar physiological consequences in photosynthetic cells (Fernández-Marín *et al.*, 2018b; Verhoeven *et al.*, 2018) the tolerance to freezing has greatly been understudied in lichens in comparison to other organisms (Bjerke, 2011; Nowak *et al.*, 2018). This could be explained because (i) as poikilohydric organisms lichens are assumed to withstand low temperatures when dry (Gauslaa & Solhaug, 1999) and (ii) because some species (from boreo-alpine and polar regions, mainly) are capable of C assimilation at sub-zero temperatures (Kappen & Lange, 1972; Kappen, 1989; Barták *et al.*, 2007). Recent works, however, have shown a great variability in the sensitivity of lichen species to freezing when wet and have evidenced an important gap

of knowledge regarding the physiological and molecular aspects involved in it (Bjerke, 2011; Hájek *et al.*, 2016; Nowak *et al.*, 2018; Solhaug *et al.*, 2018). Even if the molecular mechanisms of frost and desiccation tolerances are not fully understood in lichens (Nowak *et al.*, 2018) several studies have pointed out that the symbiosis is beneficial to the photobiont in order to counteract desiccation (Kranner *et al.*, 2005; Kosugi *et al.*, 2009), while others have highlighted the capability of the free-living photobiont to withstand low temperature and/or desiccation, particularly within the genus *Trebouxia* (Sadowsky & Ott, 2012; Candotto Carniel *et al.*, 2015).

Overall, the complex relationship among the components of the lichen consortium hinders the understanding of their separate physiologies and thus, of the physiological consequences of the symbiosis for the individual partners. Until now, major advances in their understanding are a result from studying isolated symbionts cultured under laboratory conditions. Valuable information has been obtained through this approach regarding different aspects of photobiont ecophysiology: e.g. cell osmolarity (Kosugi *et al.*, 2014), nutrient uptake (Pavlova *et al.*, 2017), photochemistry (Guéra *et al.*, 2016) or, more recently, water relations (Centeno *et al.*, 2016; Banchi *et al.*, 2018). Field studies would still be needed to completely understand the ecophysiology of lichen photobionts in their free-living forms. Nevertheless, their sparse presence in the environment and the fact of being usually cohabiting with many other taxa of microflora –e.g. on the surface of other lichen species thalli (Muggia *et al.*, 2013)– make the study of free-living photobionts an extremely challenging task under natural conditions.

A unique opportunity though, arises from the study of the exceptional association established by the lichen-forming fungus *Mastodia tessellata* (Hook. f. & Harv.) Hook. f. & Harv. (Verrucariaceae) and its photobiont, a green alga of the genus *Prasiola* (C. Agardh) Meneghini (Prasiolales, Trebouxiophyceae). Two main reasons for that are: (i)

the macroscopic and multicellular nature of the photobiont, the only known case, together with *Turgidosculum ulvae* (M. Reed) Kohlm. & E. Kohlm., of a fungus forming a lichen symbiosis with a blade-like alga (Pérez-Ortega *et al.*, 2018), and (ii) the apparent coexistence of free-living and lichenized forms of *Prasiola* in the same microenvironments (Huiskes *et al.*, 1997a) (see also Fig. 1). The characteristic symbiosis formed by *M. tessellata* has repeatedly attracted the attention of the scientific community. The species occurs on the upper littoral zone at high latitudes of both hemispheres, with extant populations in Alaska (USA), British Columbia (Canada), Tierra del Fuego (Chile), New Zealand, Tasmania (Australia), Antarctica and the subantarctic islands (for a more detailed distribution area see Garrido-Benavent *et al.* 2018). Pérez-Ortega *et al.* (2010) studied the phylogenetic affinities of both symbionts, and dismantled the monotypic family Mastodiaceae, showing that *M. tessellata* is closely related with marine members of the family Verrucariaceae. These authors also thoroughly characterised the interactions between both symbionts at the ultrastructural level, revealing a particular kind of fungal haustoria not previously observed, and pointing to a non-parasitic relationship but a rather dynamic equilibrium in which the photobiont can occasionally escape from the mycobiont. More recently, it has been shown that there are more than one species of *Prasiola* algae forming lichen symbioses with *M. tessellata* (Garrido-Benavent *et al.*, 2017). The known bipolar distribution of the lichen-forming fungus and its photobionts is the result of a complex past events, with relatively recent joint dispersal from the southern hemisphere to the northern hemisphere (Garrido-Benavent *et al.*, 2018).

To the best of our knowledge, *in situ* comparison (in Antarctica) of free-living vs lichenized *Prasiola* (e.g. *M. tessellata*) was only done before by Huiskes *et al.*, 1997*a*. Huiskes and co-workers showed that subjection to prolonged hydration was detrimental

for the photosynthetic rates of the lichen but not of the free-living *Prasiola* specimens (Huiskes *et al.*, 1997a). With a broad combination of methodologies and by integrating *in situ* and *ex situ* measurements, we aimed to address three different aspects of photobiont physiology: (1) what the differences in photosynthetic performance of co-occurring populations of free-living and lichenized *Prasiola* are; (2) to which extent the symbiosis influences the water relations in *Prasiola*, including its tolerance to desiccation; and (3) how the association affects survival and performance of *Prasiola* to sub-zero temperatures.

MATERIALS AND METHODS

Field site

Co-occurring samples of lichenized and free-living *Prasiola* (Fig. 1A–C) were measured and/or collected in Livingston Island, South Shetland Islands (62º 40'S, 60º 23'W), near the Spanish Antarctic Research Station 'Base Antártica Española Juan Carlos I (BAE JCI)' (for further details on the Base location see Laguna-Defior *et al.*, (2016)) during summer 2018 (23rd of February to 6th of March). Both *Prasiola* forms were growing on a rocky substrate in Argentina Cove, close to a gentoo penguin colony (*Pygoscelis papua* Forster) (Fig. 1C). Intermediate forms between a completely free living *Prasiola* and the lichen *Mastodia tessellata*, as described by other authors (Huiskes *et al.*, 1997b; Pérez-Ortega *et al.*, 2010), were observed but avoided during field measurements and collections. Measurements took place in austral summer 2017-2018, and the weather was characterised by a mean air temperature of 2.3 °C, with a range of variation between 10.6 °C and –5.5 °C, and with a small daily thermal amplitude (3.3 °C) (Fig. 1D). Freezing temperatures only occurred at the beginning and end of the season, and were particularly noticeable in March. Rainfall summed 173 mm during the three summer months (21st Dec to 21st March), and with no rain during only one third of the days (less than 0.1 mm) (Fig.

1D). The study period (February 25th to March 10th) was characterised by two contrasting situations (Fig 1E). The first week was pretty much comparable to the average summer trend (mean air temperature 2.5 °C, humid and cloudy), while the second week was colder (0.7 °C) and abundant in clear sunny periods (Fig. 1E). All meteorological data were kindly provided by the Spanish Agency of Meteorology (AEMET).

Identity of free-living and lichenized Prasiola

Identification of *Prasiola* specimens is usually not a straightforward task due to the reduced number of available taxonomic characters and the presence of cryptic species (Moniz *et al.*, 2012). We used a fragment of the ribulose-1,5-bisphosphate carboxylase/oxygenase large subunit gene (*rbc*L) which has been used in recent studies to infer phylogenetic relationships in the genus (Moniz *et al.*, 2012) and to reconstruct the complex evolutionary history of photobionts associated with *M. tessellata* (Garrido-Benavent *et al.*, 2017). Ten samples (5 lichenized, 5 free-living) were analysed for molecular identification. A small fragment (c. 1 mm^2) of sample cleaned under a dissecting microscope to avoid epiphytic algae was removed with a razor blade and checked under the light microscope. DNA extraction was carried out using the EZNA® Forensic kit (VWR, Spain) following manufacturer instructions. Amplification was carried out using the primer pair *rbc*L-pras-F and *rbc*L-pras-R (Garrido-Benavent *et al*. 2018). PCR reactions were performed in a total volume of 15 µL, containing 2µL of template DNA, 0.5µL of each primer (10 µM), 6.5 µL of MyTaq Mix (MyTaq DNA Polymerase (Bioline) and dNTPs); distilled water was added to reach the final volume. PCR amplifications were performed in an Eppendorf Mastercycler EP gradient S thermal cycler. PCR conditions followed Garrido-Benavent *et al.* (2018). PCR products were purified using ExoSAP-IT™ PCR Product Cleanup Reagent (ThermoFisher) according

to the manufacturer's instructions and sequenced by Macrogen Inc. (Madrid, Spain) using the same primer sets as for PCR amplification. Sequence contigs were assembled using SeqMan v.14 (Lasergene, DNA Star Inc., WI, USA).

Experimental design

The combination of physiological measurements in the field, with physicochemical and biochemical analyses in the BAE JCI and UPV/EHU laboratories allowed an in depth ecophysiological comparison of free-living and lichenized forms of *Prasiola*. Alongside the aims of the work, three main experiments were conducted as follows:

Experiment 1: To evaluate the differences in photosynthetic performance of co-occurring populations of lichenized vs. free-living specimens of *Prasiola* we combined (i) analyses of photochemical performance and photosynthetic pigments composition under natural conditions in the field, with (ii) gas exchange measurements of freshly collected wet samples under controlled conditions in the labs of the BAE JCI (Figs. 2–4). The assessment of photochemical and photosynthetic pigment adjustments in response to natural irradiance was conducted *in situ* in intact thalli of both species, in their natural microenvironment. The actual yield of PSII (YII), sample temperature and photosynthetic photon flux density (PPFD) were recorded in the field under diverse irradiance conditions and the samples preserved (fast-dried as described in Esteban *et al.* (2009)) for posterior analysis of photosynthetic pigments. Three measurements per species and time-point were conducted in a total of 23 time points with different PPFDs during the days: Feb 27, Feb 28, March 2, March 3, March 4, March 5, March 7, March 8 (Fig. 1E, green lines). Further details on chlorophyll fluorescence, gas exchange and pigment analyses are explained thereafter in specific subsections within Materials and Methods.

Experiment 2: was conducted to evaluate the influence of the symbiosis in the water relations of *Prasiola*, including its tolerance to desiccation. With this purpose pressure-volume (P-V) curves and a desiccation experiment were conducted at the BAE JCI, and an additional set of samples was collected, silica-gel dried and used to assess glass transition temperatures (Tg) and hydrophobicity of thalli surfaces in the UPV/EHU laboratories (Figs. 5–6). The desiccation experiment was performed by equilibrating freshly collected free-living and lichenized samples at 10%, 50%, 80% and 100% RH for 48 h, in darkness, at natural temperatures outdoor (≈ +4 ºC, data from AEMET station at the BAE JCI, for the days of the experiment 2-4th March 2018, Fig. 1). With an adaptation of the method described in López-Pozo *et al.* (2019) incubations were performed in 1L volume hermetic boxes containing 200 mL of silica gel (to get 10% RH), of $MgCl_2$ solution (1.87 g of $MgCl_2$ hexa-hydrated per mL of Milli-Q water, to get 50% RH), of NaCl saturated solution (80% RH), or of distilled water (100% RH). The equilibrium RH within the hermetic boxes was tested with an RH and T datalogger EL-USB- 2-LCD+ (LascarElectronics, UK). Solutions were adsorbed on a commercial kitchen sponge (Spontex Natura ®) separated from the samples by a plastic mesh and the samples were placed over petri dishes so that direct contact with the solutions was prevented. Boxes were covered with aluminium foil (to assure darkness) and located outdoor in the shade, prevented from any overheating by direct sun. Incubation was conducted for 48 h. To assess the changes in photosynthetic pigments induced by the different incubations samples were collected after 48 h and immediately frozen in liquid N_2. Maximal photochemical efficiency of PSII (F_v/F_m) was monitored before incubation and after 48 h. Additionally, a separate set of samples desiccated at 50% RH were monitored during rehydration at 0, 2, 5, 10, 20, 30 min and at 1, 6, 12, 24 and 48 h, for detailed analysis of F_v/F_m recovery. A last set of silica-gel dried samples was preserved for further analyses

in the UPV/EHU: P-V curves, Tg estimation and evaluation of thalli hydrophobicity. Detailed information on these measurements is given in specific subsections within Materials and Methods.

Experiment 3: In order to assess how the lichen symbiosis affects survival and performance of *Prasiola* at sub-zero temperatures, a controlled freezing experiment was conducted in the BAE JCI laboratories and a second sample set was used for the assessment of freezing-temperature at the UPV/EHU labs (Fig. 7). For the freezing experiment, freshly collected wet samples were acclimated to darkness for 12 h and subsequently incubated at –20 ºC, for 48 h. Changes in photosynthetic pigments were analysed before and after the freezing, and F_v/F_m monitored during incubation at –20 ºC and during the re-warming at +20 ºC. The experiment was performed in darkness. Further details on the assessment of ice nucleation temperature are specified later on in a specific subsection within Materials and Methods.

Whenever required in any of the experiments, controlled hydration was conducted with distilled water since previous works showed that *P. crispa* and *M. tessellata* are salt-tolerant but not obligate halophytes, being hypo-osmotic water undamaging for them (Jacob *et al.*, 1991; Smith & Gremmen, 2001a).

Chlorophyll fluorescence

Two types of measurements were conducted with a portable modulated Plant Stress Kit Fluorometer (PSKF, Opti-Sciences, Hudson NH, USA): YII measurements in the field and F_v/F_m in the BAE JCI lab. The maximum Chl *a* fluorescence under solar radiation (F_m') was induced with a saturating pulse of 0.8 s and 7000 µmol m^{-2} s^{-1}). The actual efficiency of PSII (YII) was estimated as YII= (F_m'-F_s)/F_m', where F_s is the actual Chl *a* fluorescence under solar illumination. The saturation pulses for F_m' estimation were

applied as described by (Loriaux *et al.*, 2013). Maximal photochemical efficiency of PSII (F_v/F_m) was assessed in dark-adapted samples in the lab for Experiments 2 and 3.

Gas exchange measurements

Net assimilation of CO_2 (A_n) was determined by using a GFS-3000 gas exchange system coupled with a fluorometer IMAGING-PAM (Heinz Walz, Effeltrich, Germany). The blue light source provided by the manufacturer, with a maximum emission at 420 nm, was used during fluorescence and gas exchange measurements. Full-hydrated samples (n = 4-5) were introduced in a custom-made cuvette consisting of a gasket stuck to a thin polyester piece of clothes. The size of the used gaskets equals the chamber ones, so that proper closure of the chamber was possible and the CO_2 leakage was close to zero. A similar sample size was used for all replicates of *M. tessellata* and *P. crispa* (3.6±0.3 and 3.6±0.2 cm^{-2}, average ± SE, respectively). Fresh weight (FW) and dry weight (DW) were individually recorded for each replicate (*M. tessellata* 77±5 and *P. crispa* 16±2 mg DW on average). CO_2 concentration was standardized at 400 ppm, relative humidity at 75-85 % and the flow rate within the chamber was 750 $\mu mol \cdot s^{-1}$. Sample temperature was set to +20 ºC, which has previously shown as optimum for maximum CO_2 assimilation rate in *M. tessellata* (Smith & Gremmen, 2001b). A_n was recorded at steady-state conditions when diffusion limitations due to interstitial water were null and biochemistry was full-light-temperature adapted (3-5 min). Ten different light intensities (0, 20, 40, 75, 165, 370, 580, 922, 1465 and 1855 $\mu mol \cdot m^{-2} \cdot s^{-1}$) were set in order to obtain a light curve. If needed, full rehydration of the sample during the light curve was done in order to avoid its desiccation by immersing in distillate water for 1-2 min and removing gently the excess of water with a paper tissue before storing the sample in the cuvette again. The negative A_n at 0 of irradiance (I) was considered the dark respiration value (R_d). The

maximum light-saturated A_n (A_{sat}) and the apparent quantum efficiency (AQE) were obtained by fitting each light curve to Michaelis-Menten (Ritchie & Prvan, 1996a,b), rational (Smith, 1936), exponential (Goudriaan, 1982) or hyperbolic tangent (Jassby *et al.*, 1976) models by using the Microsoft Excel Solver tool (Lobo *et al.*, 2013). The lowest square sum errors were obtained with Michaelis-Menten model (eqn 1).

$$A_n = \frac{A_{sat} \cdot I}{A_{sat}/AQE + I} - R_d \quad (1)$$

Calculation of the light compensation point at which A_n equals zero (I_{com}), and the irradiance at which a 90% of A_{sat} is achieved (I_{sat90}) was done for Michaelis-Menten model (eqn 2, 3).

$$I_{com} = \frac{A_{sat} \cdot R_d}{AQE(A_{sat} - R_d)} \quad (2)$$

$$I_{sat90} = \frac{A_{sat}(9A_{sat} + R_d)}{AQE \cdot A_{sat} \cdot R_d} \quad (3)$$

Photosynthetic pigment and tocopherol analysis

Photosynthetic pigments and tocopherols were analysed by HPLC following the method described by García-Plazaola & Becerril (1999, 2001) with small modifications. Briefly, approximately 10 mg of dry weight (DW) of thalli were used per replicate, and 3 to 4 replicates per treatment and/or time point for photosynthetic pigment analysis. Samples were immediately frozen in liquid nitrogen in the field after treatment and freeze-dried before analysis. Samples were doubly extracted in 0.25 mL of cold (+4˚C) Acetone:Water (95:5 v:v) first, and in 0.25 mL of pure acetone second. All acetone solutions were buffered with $CaCO_3$. Both supernatants were filtered through a 0.2 µm polytetrafluoroethylene filter (Teknokroma, Barcelona, Spain) before being analysed by

HPLC. Tocopherol and pigments detection and quantification were conducted with a scanning fluorescence detector Waters 474 operating in series with a photodiode array detector Waters 996 (Waters, Milford, MA, USA) (García-Plazaola & Becerril, 1999, 2001). The relative de-epoxidation state of the xanthophyll cycle pigments was estimated by the ratio (Antheraxanthin + Zeaxanthin) / (Violaxanthin + Antheraxanthin + Zeaxanthin), abbreviated as "AZ/VAZ".

Water potential measurements

Sample water potentials were determined with a dewpoint hygrometer (WP4, Decagon Devices, Pullmann, WA, USA) in the laboratory of the BAE JCI, following similar protocol as previously used for bryophytes and lichens (Proctor *et al.*, 1998; Nardini *et al.*, 2013; Petruzzellis *et al.*, 2018). The instrument was calibrated at the beginning of each measurement session using 0.5 M KCl standard solution. The fully hydrated thalli (equilibrated for 24 h at 100% RH over wet paper) were measured for their initial water potential (Ψ) and immediately weighed to determine the initial fresh weight. Samples were left to dry on the lab bench at 50% RH and 22-24 ºC, and Ψ measured subsequently at different times during dehydration. After each reading, samples were immediately weighed to match each Ψ to the corresponding weight. At the end of the measurements, each sample was dried in the oven at 70 ºC for 24 h to determine their DW. Absolute and relative water contents (WC, RWC) were then calculated for each sample and time point.

Typical P-V curves were obtained by plotting the 1-RWC values (x-axis) against the corresponding $-1/\Psi$ (y-axis). Two phases were distinguished during desiccation of samples: in the first phase, small changes in Ψ occurred with high losses of water from the samples until the turgor loss point (TLP) was reached. In a second phase, which

corresponds to values below TLP, the curve became linear ($r^2 > 0.98$). The y-axis intercept of the linear portion of the P-V curve is the reciprocal of the full-turgor water potential (Ψo). The point at which the linear portion of the curve begins to curve upwards towards the y-axis is the turgor-loss point (TLP); the points between TLP and the y-axis provide the data for calculating cell wall elasticity, known as modulus of elasticity (ε). The following parameters were calculated according to Sack *et al.*, (2011): water content at full turgor (saturated water content: SWC, $gH_2O \cdot g^{-1}$ DW) and at TLP (RWC_{TLP}, %), osmotic potential at full turgor (Ψo, MPa), water potential at the turgor loss point (Ψ_{TLP} , MPa), and modulus of elasticity (ε, MPa). Specifically, the "water mass at turgor" was estimated as the intercept of sample water mass and Ψ at which Ψ equals zero. Then, the SWC was calculated as "water mass at turgor"/DW, and one value was obtained per sample. The RWC was estimated as (FW-DW)/(TW-DW)*100 being TW-DW="water mass at turgor", and several data points were obtained for each sample during the desiccation process.

Molecular mobility

Mechanical analyses were conducted on desiccated thalli (equilibrated with silica gel) of lichenized and free-living *Prasiola*, in order to estimate how lichenization affects molecular mobility of dry thalli. These measurements provide information about the extent of molecular mobility (and thus the potentiality of enzymatic activity) at a wide range of temperature (Ballesteros & Walters, 2011). A Dynamic Mechanical Thermal Analyser (DMA/SDTA861e, Mettler Toledo, Greifensee, Switzerland) in the shear mode was used for the mechanical analysis. The method is similar as described in (Fernández-Marín *et al.*, 2013) with the modifications described in (Fernández-Marín *et al.*, 2018*b*). Briefly, measurements from –50 to +150˚C at a heating rate of 2˚C min^{-1} were carried out

in the dynamic mode. Each sample was scanned twice. Three biological replicates, of approximately 300 mg DW each, were measured per species. Shear storage modulus (G´), shear loss modulus (G") and the loss tangent (tanδ = G"/G´) were calculated using the Mettler Toledo START^{e} software during dynamic mechanical thermal analysis (DMTA) scans. For each biological replicate, the temperature value at the maximum tanδ coincident with the alpha-relaxation measured at 1Hz, was consider for Tg estimation.

Hydrophobicity of the thallus surface

The contact angle of droplets of distilled water was measured over thalli equilibrated with silica gel in order to estimate the hydrophobicity of their surface, following a similar method as previously used for lichens (Hauck *et al.*, 2008). Measurements were conducted with a video-based Optical Contact Angle measuring instrument (OCA 15EC, from DataPhysics Instruments GmbH, Filderstadt, Germany). Sessile droplets of 3 µL were placed on the upper side of the thalli. The contact angle was estimated with the SCA software for optical contact angle, v.4.4.3. The measuring precision was of ± 0.1º. Measurements were performed in 10 different thalli per species at one second after contact. Each value was the mean from the optically left and right margins of the water droplet.

Determination of ice nucleation (freezing) temperature

The freezing temperature of lichenized and free-living *Prasiola* samples was analysed with a Differential Scanning Calorimeter (DSC 822e from Mettler Toledo, Greifensee, Switzerland) at full turgor, in ≈10 mg size thalli following a similar method as described in Fernández-Marín *et al.*, (2018*b*). Full turgor samples were sealed in aluminium pans and characterized under constant liquid nitrogen flow (20 mL min^{-1}).

First, samples were equilibrated at 0˚C and then cooled at a rate of 0.1˚C·min^{-1} from 0˚ to –15˚C. Subsamples of the same set used for DSC scans were used to estimate absolute water content. Before the measurements, the DSC equipment was calibrated with zinc, indium and pure water as standards. All weights were recorded using a Mettler Toledo 0.1 mg precision balance. DSC measurements were performed in at least five different thalli per species.

Statistics

Normal distribution of data was checked with the Kolmogorov-Smirnov test and homogeneity of variances with Levene test. One-way ANOVA was used to test for differences between lichenized and free-living forms of *Prasiola* in each of the analysed parameters: pigment contents, WC, F_v/F_m, glass transition and freezing temperatures, contact angle, and parameters derived from P-V curves and from gas exchange modelling. When data showed heteroscedasticity, the non-parametric test Kruskal-Wallis was used. Statistical analyses were conducted with SPSS v24.0 and significant levels considered at α=0.05.

RESULTS

Identification of Prasiola species

Sequences recovered from free-living and lichenized co-occurring samples of *Prasiola* in Argentina Cove showed that they corresponded to two different species. All sequences gathered from lichenized *Prasiola* were identical, and 100% matched with *Prasiola* sp. in blast searches (Altschul *et al.*, 1997), a putative new species previously reported from other lichenized *Prasiola* samples from Antarctica (Garrido-Benavent *et al.*, 2017).

Sequences from free-living specimens were almost identical (differing only in 5 positions) and all matched either 100% or 99% with *Prasiola crispa* in blast searches.

Photochemistry

Figure 1E shows the meteorological conditions (RH, temperature, and more importantly, irradiance) during the measurements of YII and the collection of samples for the subsequent analyses of photosynthetic pigments and tocopherols. The extension of the study period allowed us to get a detailed picture of the response of photochemical parameters to the environmental constraints, e.g. a wide range of irradiances was covered. Figure 2 shows the average content of photosynthetic pigments and tocopherol of samples that were directly preserved in liquid nitrogen in the field. Lichenized and free-living *Prasiola* did not differ qualitatively in their pigment and tocopherol composition. All major carotenoids typical from green photosynthetic organisms, including the not always present α-Carotene (α-Car), were found, and α-tocopherol (α-Toc) was the only isoform of tocopherol identified in both species. Nevertheless, several differences were found in the quantitative contents of photosynthetic pigments. The free-living *P. crispa* showed significantly higher content of Chl when expressed per DW and significantly lower Chl a/b ratio (Fig. 2A, B). The free-living *P. crispa* also showed lower thallus mass area (TMA) than *M. tessellata* (45±4 vs 224±27 g m^{-2}, data not shown) and a predominantly mono or di-stromatic structure with a higher concentration of photosynthetic cells (Supplementary data Fig. S1). Its lutein (Lut) and β-Car to Chl ratios were higher and its neoxanthin (N) to Chl ratio lower than in the lichenized form (Fig. 2C–H). No significant differences were found in the xanthophyll cycle pigments nor in the α-Toc content between both species (Fig. 2E, F, I). Interestingly, the de-epoxidation index of xanthophyll cycle in these field-sampled thalli was always above 0.4 for both species.

An exhaustive sampling of actual photochemical efficiency (YII) along ten days of measurements was conducted *in situ* (Fig. 3; the exact data points are highlighted as green lines in Fig. 1E). This allowed a detailed characterization (n=122 datapoints per species) across a good representation of the natural irradiance range occurring in the microenvironment of both *Prasiola* forms: from 22 to 1679 µmol photons m^{-2} s^{-1} (Fig. 3A, B). The variability of YII values, particularly at lower irradiances, reflects the potential range displayed for both species as for instance depending on water availability (see also Fig. 3C, D). Light responses were photochemically similar between both species that showed saturation PPFD at around 600 µmol photons m^{-2} s^{-1}. Interestingly, free-living *P. crispa* showed higher YII than the lichenized form *Prasiola* sp. at low PPFD below ≈200 µmol photons m^{-2} s^{-1} (Fig. 3A, B). The trend of photosynthetic pigments in response to last-week precipitation and cumulative irradiance was also evaluated (Fig. 3C, D). While both species responded similarly, it was remarkable an increasing (although not significant) trend in the AZ/VAZ in response to higher cumulative irradiance (Fig. 3C) and a decreasing trend in response to higher cumulative precipitation (Fig. 3D).

Gas exchange

A_{sat} was 47.1 % higher in the free-living alga (Fig. 4B), as a result of an increased dark respiration due to fungal contribution in the lichen (R_d of 1.61 ± 0.12 µmol CO_2 m^{-2} s^{-1}, mean ± SE) than in the free-living *P. crispa* (0.47 ± 0.07) (Fig. 4C). Net carbon assimilation in response to irradiance was very similar between both species on a thallus area basis (Fig. 4). By contrast, due to dissimilar TMA and chlorophyll content of the two species (see above), the were accentuated when expressed on a biomass basis (Supplementary data Figs S2, S3). Thus, A_{sat} was seven fold higher in *P. crispa* than in

M. tessellata on a Chl basis (Supplementary data Fig. S3B) and nine fold higher on a DW basis (Supplementary data Fig. S2B). Rd (on a Chl basis) was not significantly different between both species (Supplementary data Fig. S3C) but was higher in *P. crispa* when expressed on a DW basis (Supplementary data Fig. S2C). I_{com} was significantly higher in the lichen (78.5 ± 11.9 µmol photons m^{-2} s^{-1} compared to 12.8 ± 2.3 in *P. crispa*, Fig. 4E) and, I_{sat90} was accordingly achieved at higher irradiances (Fig. 4D). Both species showed an equal AQE (data not shown). A similar trend occurred when light curves were performed at +10 ºC with an expected displacement towards lower I_{com} and I_{sat90} (Supplementary data Fig. S4).

Water relations and tolerance to desiccation

Pressure-volume curves and corresponding estimated parameters for thalli of *M. tessellata* and *P. crispa* are shown in Fig. 5. Both osmotic and water potentials at turgor were lower in *M. tessellata* than in *P. crispa*: Ψo= –1.9MPa ± 0.8 vs –0.9 ± 0.0; and Ψ_{TLP}= –3.6 ± 0.1 vs –2.6 ± 0.1, respectively (Fig. 5C, D). Interestingly, the water content at saturation in *P. crispa* (SWC= 2.7 ± 0.0 g H_2O g^{-1} DW) was two-fold higher than in *M. tessellata* (1.4 ± 0.1; Fig. 5E). The modulus of elasticity was also very distinct between both species being 3.5-fold higher in *M. tessellata* (3.8 ± 0.0 MPa) than in *P. crispa* (1.1 ± 0.1 MPa, Fig. 5F). Remarkably, turgor loss point occurred at significantly higher RWC in *M. tessellata* (RWC_{TLP}= 60 ± 1 %) than in *P. crispa* (42 ± 1, Fig. 5G). Capacitance at full turgor was significantly higher in *M. tessellata* (C_{FT}).

Further parameters related to water relations and to the capacity to counteract cell dehydration are shown in Fig. 6. Controlled desiccation by equilibrium at three different RHs, in darkness, led to different final water contents (e.g. desiccation extents) of >0.2, around 0.1 and <0.1 g H_2O g^{-1} DW in both species (Fig. 6A). All samples were able to

recover their initial F_v/F_m values after 48 h of rehydration indicating a comparable tolerance to short-term (48 h) desiccation in *Prasiola* sp. and *P. crispa* regardless the severity of the dehydration reached (Fig. 6B). The incubation in darkness induced a slight increase in the de-epoxidation level of both species although without significance (Fig. 6C). The mechanical analysis of samples equilibrated at 10% RH revealed that both species were in the glassy state (e.g. with severely reduced molecular mobility) at ambient temperature (e.g. 4 ºC) since their glass transition temperatures (Tg) were one order of magnitude higher (above 40 ºC, Fig. 6D). The average Tg was remarkably higher in *M. tessellata* than in *P. crispa* (52.2 ± 4.4 and 45.1 ± 1.0 ºC, respectively) but both *Prasiola* species were able to completely recover photochemical efficiency upon rehydration (Fig. 6E). The contact angle of distilled water droplets over *P. crispa* thalli was on average significantly lower than over *M. tessellata*. This was indicative of significantly higher hydrophilicity in the free-living *P. crispa* (Fig. 6F).

Freezing tolerance

The evolution of F_v/F_m and xanthophyll cycle pigments during a controlled freezing treatment of wet thalli is shown in Figure 7A, B. A slow but progressive decrease in F_v/F_m was observed along the 48 h of incubation at –20 ºC in both species (Fig. 7A). This decrease was remarkably slower in the lichenized *Prasiola* sp. that kept significantly higher values than *P. crispa* during the first 24 h of incubation. In agreement with this, the recovery of F_v/F_m values during the re-warming at +20 ºC, was also faster in the lichenized *Prasiola* sp. with significantly higher values along the first 30 min. Both species notably recovered their photochemical activity in the extremely short time laps of 6 hours during rewarming to +20 ºC: the % to the initial value was 107 ± 2 in the lichenized *Prasiola* sp and 97 ± 3 in *P. crispa* (average ± SE, Fig. 7A). An increasing

trend towards higher de-epoxidation levels was obtained in the thalli at the end of the freezing treatment (of around 30% increase in *M. tessellata* and of ≈10% in *P. crispa*), although without statistical significance (Fig. 7B). According to the observed behaviour in F_v/F_m, the average ice nucleation temperature (in ºC) was significantly lower in the lichen –7.1 ± 0.4 than in the free-living *P. crispa* –5.1 ± 0.4 (average ± SE, Fig. 7C, see also Supplementary data Fig. S4). Thalli of both species subjected to –20 ºC in the dry state recovered relatively faster than wet samples, during rehydration at +20 ºC, with no significant differences between both species (data not shown).

DISCUSSION

Lichenized and free-living Prasiola *populations co-occur in Polar Regions*

The identity of the photobiont of *Mastodia tessellata* as *Prasiola crispa* subsp. *antarctica* and the co-occurrence of free-living and lichenized forms of this species in Antarctica have been long-standing tenets (Huiskes *et al.*, 1997*a*,*b*; Lud *et al.*, 2001*b*). Recently Moniz *et al.* (2012) resurrected *P. antarctica* Kützing as an independent species, almost morphologically indistinguishable from *P. crispa* (Lightfoot) Kützing but molecularly distinct. Garrido-Benavent *et al.* (2017) studied lichenized *Prasiola* populations from the northern and southern Hemisphere, including Antarctica, and concluded that while Tierra del Fuego and most of the Alaskan specimens belonged to the species *Prasiola borealis*, most lichenized *Prasiola* specimens from Antarctica corresponded to an undescribed species, not known so far as free-living. Subsequently, Garrido-Benavent *et al.* (2018) showed in a thorough analysis that *P. borealis* from Tierra del Fuego and *Prasiola* sp. from Antarctica diverged around middle to latest Miocene coinciding with the opening of Drake Passage. In our study, we found that the two co-occurring *Prasiola* forms belong to two different species: free-living specimens corresponded to *Prasiola crispa* and

lichenized to *Prasiola* sp. The former is a nitrophilic species that usually grows close to penguin rookeries (Graham *et al.*, 2009) and is known from both hemispheres (Moniz *et al.*, 2012). On the other hand, *Prasiola* sp. is, so far, only known in the lichenized form and from Antarctica (Garrido-Benavent *et al.*, 2017, 2018). The fact that co-occurring forms of *Prasiola* do not belong to the same species as previously thought raises the questions of what the niche of free-living *Prasiola* sp. is and whether it does really occur free-living. *Prasiola borealis*, the most common photobiont of *M. tessellata* out of Antarctica is known to occur free-living (Garrido-Benavent *et al.*, 2017), and so we expect for *Prasiola* sp., although it may happen that it occupies a different niche when free-living as it is known for other photobionts (Sanders *et al.*, 2004).

Effect of lichenization in the photosynthetic performance of Prasiola

Both lichenized and free-living specimens showed similar photosynthetic performances with lower net assimilation rates in the lichenized growth form on a thallus area basis (Fig. 4). This is most likely a result of higher energy consumption and respiratory carbon loss deriving from the mycobiont. Dark respiration rates were 4-fold higher than that from the photobiont in its free-living growth form (Figs. 4A, C). The carbon assimilation of *M. tessellata* and different species of *Prasiola* have been previously reported (Smith & Gremmen, 2001*a*,*b*; Kang *et al.*, 2013; Holzinger *et al.*, 2017). Nevertheless, and as far as we are concerned, photosynthesis data of both *M. tessellata* and *P. crispa* have only been compared by Huiskes *et al*. (1997*b*) so far, at non-saturating irradiation and low temperature. At those conditions, *P. crispa* also showed higher A_n than *M. tessellata*. Photosynthetic capacity of *M. tessellata* was unaffected by low temperatures (from +5 to +20ºC) meanwhile $R_{d,}$ and I_{com} decreased (Smith & Gremmen, 2001*a*,*b*). Although A_{sat} and I_{sat90} decreased in the lichenized form (Fig. 4B,

D), it should not be interpreted as a lower capacity of the photobiont to consume or deal with excess light, since AQE remains equal to the free photobiont and the fungal respiration can explain most of the modulation of both parameters. Indeed, the actual irradiance reaching photosynthetic cells in the lichen is, very likely, reduced by the melanised upper cortex and by the thicker thallus (Supplementary data Fig. S1). If data are though normalised by Chl content, the lichenized *Prasiola* appears as much less efficient in terms of A_N (Supplementary data Fig. S3). This could be explained by (i) the pluri-layered structure of the lichenized algae (Supplementary data Fig. S1) related with a higher Chl content on a thallus area basis, and (ii) by the fungal biomass.

Lichenized and free-living forms of *Prasiola* showed very similar photosynthetic response to changing light conditions (Fig. 4). In agreement with this, photochemical efficiency (YII) measured in the field responded very similarly to irradiance in *P. crispa* and lichenized *Prasiola* sp. (Fig. 3A). The main difference was observed at low irradiance (e.g. PPFD<200 µmol m^{-2} s^{-1}) at which *P. crispa* showed higher YII (Fig. 3A), possibly due to a difference in its alternative sink of electrons pathways, since both *P. crispa* and *M. tessellata* presented equal AQE for CO_2 fixation. At higher irradiances (>600 µmol m^{-2} s^{-1}) both species showed similar YII (≤0.1) but much higher I_{sat90} was shown by *P. crispa* (Fig. 4D). This could be related to efficient photoprotection mechanisms. *Prasiola crispa* seems to be rather tolerant to UV (Post & Larkum, 1993; Holzinger *et al.*, 2006) and *Mastodia tessellata* has also been shown to be very tolerant even to UV-B (Lud *et al.*, 2001a). Both intensity and quality of irradiance affect photo-inactivation of PSII, and while no data are available for *M. tessellata*, so far, a newly identified desiccation-induced protection mechanism that prevents inactivation of the oxygen evolving complex under severely reduced water contents has recently been evidenced in Antarctic *P. crispa* (Kosugi *et al.*, 2018).

Chlorophyll content per thallus dry weight was 22.6% lower in *M. tessellata* than in *P. crispa* (2.8±0.2 vs 3.6±0.3 μmol g^{-1} DW, average ± SE, Fig 2A). Thallus mass area (TMA) of *M. tessellata* was, on average, 5-fold the TMA of *Prasiola*. Assuming a similar Chl content in free-living and symbiotic *Prasiola* this would indicate that the mycobiont contributes to only one fifth of the lichen biomass. This contribution of the mycobiont to the lichen biomass could be even lower if a reduction in the Chl content per area is assumed to be caused by the deterioration of some algal cells with massive penetration of fungal haustoria (Pérez-Ortega *et al.*, 2010). Interestingly, Chl a/b, usually considered as a good reported of light acclimation (the higher is the value, the higher the light acclimation) (Esteban *et al.*, 2015), was higher in lichenized *Prasiola* (Fig. 2B). This seems counterintuitive since light filtering by the fungal tissue should decrease light reaching the photobionts (Solhaug *et al.*, 2010), as it has been described previously that fungal hyphae form a dense network surrounding individual *Prasiola* cells (Pérez-Ortega *et al.*, 2010) and that the outermost layer of the thallus contains melanin (Lud *et al.*, 2001*b*). This fact could be explained then due to the preferences of *M. tessellata* for more exposed microhabitat or to intrinsic differences between the free-living and symbiotic *Prasiola* species. The latter scenario could also explain the existence of significant differences in the ratios to Chl of some carotenoids such as β-Car, Lut and Neo (Fig 2). Although not evaluated in this work, the ultrastructure of the plastid is very similar in the free-living *Prasiola crispa* (Holzinger *et al.*, 2006) and the lichenized form *M. tessellata* (Pérez-Ortega *et al.*, 2010). Very few works have dealt with the composition and dynamics of photosynthetic pigments and tocopherol in lichens generally (Demmig-Adams *et al.*, 1990; Kranner *et al.*, 2003; Fernández-Marín *et al.*, 2010; Míguez *et al.*, 2017), and these are virtually unknown at latitudes > 60º except for a couple of Antarctic lichen species (Lud *et al.*, 2001*a*; Strzalka *et al.*, 2011; Sadowsky & Ott, 2012). Our data

reveal higher α-Toc/Chl ratios (around 4-fold) than that found in temperate lichen species (Kranner *et al.*, 2003) which could be a species-specific trait or, the combined consequence of age and stress-related factors (Lizarazo *et al.*, 2010). HPLC analyses also revealed that relatively high AZ/VAZ values are continuously maintained in the field, in both species, with low re-epoxidation during nights (Fig. 1D, 2F). These elevated AZ/VAZ values only decreased after several consecutive days of either low irradiance, rain or both (Fig. 3B). Nevertheless, the capacity for faster re-epoxidation of xanthophyll cycle pigments was demonstrated, as samples artificially kept in darkness at high RH showed AZ/VAZ values of 0.15 (Fig. 6C, 7B), a value typical for dark-adapted non-stressed photosynthetic organisms (Verhoeven *et al.*, 1998). A similar lack of night relaxation of the xanthophyll cycle at high latitudes has been observed during summer in the case of other terrestrial photosynthetic organisms (Fernández-Marín *et al.*, 2018a, 2019) probably indicating an exacerbated de-epoxidation of the cycle under a long (>12h light) photoperiod.

Since lichenization has a tremendous effect in terms of carbon economy for the photobiont, the benefit of the symbiosis could be a superior resistance to environmental stress. To test this hypothesis, water relations, desiccation and freezing tolerance were studied in more detail.

Water relations and tolerance to desiccation in free-living vs lichenized Prasiola

New methodological approaches are representing new perspectives on their ecophysiological interpretation and understanding of water relations in lichens (Nardini *et al.*, 2013; Bacior *et al.*, 2017; Petruzzellis *et al.*, 2018). Compared to other lichen species *M. tessellata* showed relatively low (very negative) Ψ_{TLP}, and cell wall elasticity (e.g. high ε) (Nardini *et al.*, 2013). In agreement with Petruzzellis *et al.*, (2018), who

compared isolated photobionts to its lichenised forms, in our study *P. crispa* samples showed higher cell wall elasticity (e.g. lower ε), higher (less negative) Ψ_{TLP}, and higher Ψo than *M. tessellata* (Fig. 5). Interestingly, *P. crispa* had higher SWC and lower RWC_{TLP} than the lichen, what together with the more elastic cell wall indicates a greater water content range for the free-living algae between saturation and turgor loss points. Related to this, Bacior *et al.* (2017) have recently shown similar hydration kinetics and sorption isotherms for *M. tesselata* and *P. crispa* with the exception of a larger fraction of loosely bound water in the lichen. The presence of liquid water (more than vapour) was previously described to be beneficial for a high photosynthetic efficiency in *P. crispa* (Kosugi *et al.* (2010). A high content of easily hydrating pectinic substances in the cell wall was already proposed as a potential reason behind the water retention properties of *P. crispa* (Jacob *et al.*, 1992). It has been recently pointed out that the loss of turgor can play a key role in triggering desiccation-related responses at the photobionts cell level (Banchi *et al.*, 2018). This considered, and based on the differences in the water relations found between free living and lichen forming species, it would be reasonable to expect different physiological strategies against desiccation.

Our short-desiccation (48h) approach did not support differences in desiccation tolerance between *M. tessellata* and *P. crispa* (Fig. 6). This terrestrial alga has already been described to be desiccation tolerant (Kosugi *et al.*, 2010). The authors observed that desiccation induces a strong quenching of chlorophyll fluorescence together with a loss of PSII activity. In agreement with such study our data showed the complete inhibition of F_v/F_m in the dry state (Fig. 6E). Other species from the genus showed different extents of tolerance to desiccation. The terrestrial temperate species *P. calophylla* for example, survives equilibration to 60 % RH at least for 2 h and without alterations in the thylakoidal structure of its chloroplasts (Holzinger *et al.*, 2017) while the arctic *P. sipitata* shows high

tolerance to severe desiccation (Kang *et al.*, 2013). This same species, however, suffers deleterious effect upon long-term desiccation (e.g. 30 d) (Kang *et al.*, 2013). Long-incubation in darkness also showed damaging effects for *P. crispa* equilibrated at different RHs (Jacob *et al.*, 1992), and 96 h desiccation to 5% RH induced high mortality in an unidentified *Prasiola* incubated under the light (Davey, 1989). Glass transition temperature (Tg) of *M. tessellata* and *P. crispa* in the dry state was around 10 ºC higher than previously found for silica gel-dried mosses (Fernández-Marín *et al.*, 2013) or for resurrection angiosperms equilibrated to 50% RH (Fernández-Marín *et al.*, 2018*b*). Although not significant, a clear trend towards higher Tg was found in *M. tessellata* which could be related with lower molecular mobility and then slower deteriorative reactions (e.g. ageing) at long-term in the dry state (Fernández-Marín *et al.*, 2013). On the light of the determined Tg (Fig. 6D) and on the general assumption that tolerance to desiccation of lichen photobionts seems to be enhanced in their lichenized form (Kranner *et al.*, 2005; Kosugi *et al.*, 2009) *M. tessellata* may show better preservation of functional integrity in the dry state at a longer temporal scale. In agreement with this, Huiskes and co-workers found that continuous hydration promotes algal growth while desiccation promotes the fugal success within the delicate equilibrium of this symbiosis (Huiskes *et al.*, 1997a).

In summary, our results do not support an effect of lichenization on the desiccation tolerance of *Prasiola*, at short-term, although it may have a positive effect upon long-term (several days) desiccation events.

Lichenization enhances tolerance to freezing in Prasiola

The accumulation of the antioxidant and membrane stabilizer Zea has been reported upon desiccation and upon freezing conditions in different photosynthetic organisms including resurrection plants, lichens and intertidal macroalgae (Fernández-

Marín *et al.*, 2010, 2011*a*,*b*, 2013, 2018*b*; Verhoeven *et al.*, 2018). Although a trend towards higher AZ/VAZ was observed upon desiccation and low temperature for *P. crispa* and *M. tessellata* (Figs. 6C and 7B, respectively) no significant differences in this ratio were obtained under the used experimental conditions. Even though, F_v/F_m decreased considerably (a 90%) after 48 h of incubation at –20 ºC in both species, being this drop slower in *M. tessellata*. It is remarkable in that sense that only after incubation time longer than 24 h did the F_v/F_m drop below 50% of the initial value (Fig. 7A). By contrast, this happened in the first six h of incubation in the free-living *Prasiola* (Fig. 7A). Accordingly, ice nucleation point was significantly lower in *M. tessellata* than in *P. crispa* (Fig. 7), and 2–3 ºC lower than that reported for temperate lichen species growing at high latitudes such as *Lobaria virens* and *L. pulmonaria* (Solhaug *et al.*, 2014). The lower ice nucleation temperature in *M. tessellata* was in agreement with a slower depression in its photochemical activity along with incubation at –20 ºC and with its faster recovery upon thawing when compared to *P. crispa* (Fig. 7). While literature is available about freezing tolerance of intertidal algae, much less is known regarding lichen tolerance to freezing in their hydrated state and, to the best of our knowledge, virtually no study has dealt with the effects of lichenization on the enhancement of the photobiont fitness under low temperature. Isolated photobionts from antarctic lichens within the genus *Trebouxia* have been described as highly tolerant to freezing even when artificially isolated from their respective mycobionts (Sadowsky & Ott, 2012). *Prasiola crispa* seems to survive freezing (Jackson & Seppelt, 1995) and some species in the genus, show the ability to photosynthesise at low-temperature down to –15 ºC (Becker 1982). Despite of it, on the light of our results, it seems that the tolerance to freezing in *Prasiola* can be enhanced in symbiosis with the fungus *M. tessellata* (Fig. 7). Two potential explanations could be argued: (i) morpho-anatomical modifications induced by the presence of fungal

hyphae in the lichenized form (see Supplementary data Fig. S1) and (ii) biochemical alterations. In agreement with the former, very recent data on the water behaviour of *M. tessellata* vs *Prasiola* indicate changes in the patterns of ice crystallization induced by both structure and biochemistry of the lichenized forms (Bacior *et al.*, 2019). In agreement with the later, hardening of the photobiont against environmental constrains (such as desiccation) mediated by metabolic changes (e.g. accumulation of compatible-solutes like arabitol) upon lichenization has been evidenced for some species (Kosugi *et al.*, 2013). In a similar way the contribution of the mycobiont with cryoprotectant substances could be relevant in the protection of the lichenized *Prasiola*.

Although out of the scope of this work, other potential benefits of lichenization to the photobiont such as the reduced impact of herbivorism or pathogen infection could be considered in future studies. Interestingly, our data also represent new evidence about how free-living algae can cope with abiotic stress without any protection of the fungal partner. This has also been observed in astrobiological experiments under extreme experimental conditions (Sánchez *et al.*, 2014) highlighting the intrinsic high-stress resistance of many lichen photobionts.

CONCLUSIONS

Overall, our work provides new insights into the functioning of the symbiosis established by *Prasiola* sp. and the lichen forming fungus *M. tessellata in Antarctica*. While the lichenization appears to have no positive effect on the photochemical performance of the alga, or in its tolerance to desiccation (at short-term at least), the symbiosis represents (1) changes in its water relations, (2) a considerable decrease in net carbon uptake (due to fungal respiration and energy consumption) and (3) an enhanced tolerance to freezing. The profound impact of lichenization on the carbon balance cannot have a neutral effect,

however, there is not a clear explanation to why scattered patches of both *Mastodia* and *Prasiola* coexist in the same microsites (Fig. 1). In light of our results, enhanced tolerance to low temperature would be a relevant ecological benefit for Prasiola upon lichenization. All things considered, whether the overall changes in the functioning of the alga as a consequence of the lichenization will be reciprocally beneficial for the symbionts or will rather move towards the single benefit of one of the partners, seems to be rather dependant on environmental factors. It has already been reported that warmer winters could be deleterious for freezing-tolerant lichens (Bjerke, 2011) and that the differences in the A_n between *P. crispa* and *M. tessellata* are exacerbated under long term incubation in the hydrated state (Huiskes *et al.*, 1997b). In a climate change scenario a rise in temperature that would (i) led to depressed A_n and (ii) reduce the benefits of frost tolerance when lichenized, would very likely lead to the spread of the free-living algae in detriment of the lichen form, with resultant alterations of unknown consequences in Antarctic ecosystems.

SUPPLEMENTARY DATA

Supplementary data are available online at https://academic.oup.com/aob and consist of the following. Figure S1: details of *M. tessellata* and *P. crispa* anatomy obtained under the optical microscopy. Figure S2: gas exchange data of both species on a DW basis. Figure S3: gas exchange data of both species on a Chl content basis. Figure S4: carbon assimilation curve of *P. crispa* and *M. tessellata* measured at +10 ºC with a CMS 400 photosynthesis system. Figure S5: DSC scans of of hydrated thalli from *M. tessellata* and *P. crispa* for estimation of freezing temperature.

FUNDING

Spanish Ministry of Economy and Competitiveness (MINECO) and the ERDF (FEDER) funded the projects [CTM2014-53902-C2-2-P], [CTM2014-53902-C2-1-P], [CTM2015-64728-C2-2-R] and [CTM2015-64728-C2-1-R]; it also funded the 'Juan de la Cierva-Incorporation' post-doctoral fellowship [IJCI-2014-22489] to B. F-M.. The Spanish Ministry of Education, Culture and Sport (MECD) supported pre-doctoral fellowship (FPU-02054) awarded to A. P-C. The Spanish Ministry of Science, Innovation and Universities supported SPO through a 'Ramón y Cajal' contract (RYC-2014-16784). The Basque Government funded the projects [UPV/EHU IT-1018-16] and [UPV/EHU IT-718-13], and a pre-doctoral fellowship to M. L-P. Alexander von Humboldt Foundation is gratefully acknowledged for financial support to C. C. via the Feodor Lynen Research Fellowship.

ACKNOWLEDGEMENTS

We deeply thank the extraordinary support received at the Spanish Antarctic Research Station BAE JCI from all the staff of the "Unidad de Tecnología Marina-UTM, Campaign 2017/2018" and to the AEMET Antarctic group. With particular emphasis we would like to thank to Miki Ojeda and Joan Ribas for their outstanding disposition and efficiency in the resolution of difficulties and to José Vicente Albero Molina for kindly providing meteorological data. We also thank our colleague Miquel Nadal for kind help during weighing of samples.

Abbreviations list

AEMET: Spanish Public Agency of Meteorology ("Agencia Española de Meteorología")

Ant: antheraxanthin

A_n: net carbon assimilation

A_{sat}: maximum light-saturated irradiance

AQE: apparent quantum efficiency

BAE JCI: official abbreviation for the Spanish Antarctic Research Station "Base Antártica Española-Juan Carlos I"

α-Toc: α-tocopherol

α-Car: α-carotene

β-Car: β-carotene

C_{FT}: capacitance at full turgor

Chl: chlorophyll

DSC: differential scanning calorimeter

DMTA: dynamic mechanical thermal analyser

DW: dry weight

ε: cell wall elasticity modulus

F_v/F_m: maximal photochemical efficiency of PSII

HPLC: high performance liquid chromatography

I: irradiance

I_{com}: irradiance compensation point (irradiance at which A_n equals zero)

I_{sat90}: irradiance at which a 90% of A_{sat} is achieved

Lut: lutein

Neo: neoxanthin

Ψ: water potential

Ψo: osmotic potential

PPFD: photosynthetic photon flux density

PSII: Photosystem II

R_d: respiration in darkness

RH: relative humidity

RWC: relative water content

SWC: water content at saturation

Tg: glass transition temperature

TLP: turgor loss point

TMA: thallus mass area

UPV/EHU: official abbreviation for the University of the Basque Country

Vio: violaxanthin

YII: actual quantum yield of PSII

Zea: zeaxanthin

LITERATURE CITED

Altschul SF, Madden TL, Schaffer AA, Zhang J, Zhang Z, Miller W, Lipman DJ. **1997**. Gapped BLAST and PSI-BLAST: a new generation of protein database search programs. *Nucleic Acids Res* **25**: 3389–3402.

Asplund J, Wardle DA. **2017**. How lichens impact on terrestrial community and ecosystem properties. *Biological Reviews* **92**: 1720–1738.

Bacior M, Harańczyk H, Nowak P, Kijak P, Marzec M, Fitas J, Olech MA. **2019**. Low-temperature immobilization of water in Antarctic *Turgidosculum complicatulum* and in *Prasiola crispa*. Part I. *Turgidosculum complicatulum*. *Colloids and Surfaces B: Biointerfaces* **173**: 869–875.

Bacior M, Nowak P, Harańczyk H, Patryas S, Kijak P, Ligęzowska A, Olech MA. **2017**. Extreme dehydration observed in Antarctic *Turgidosculum complicatulum* and in *Prasiola crispa*. *Extremophiles* **21**: 331–343.

Ballesteros D, Walters C. **2011**. Detailed characterization of mechanical properties and molecular mobility within dry seed glasses: Relevance to the physiology of dry biological systems. *Plant Journal* **68**: 607–619.

Banchi E, Candotto Carniel F, Montagner A, Petruzzellis F, Pichler G, Giarola V, Bartels D, Pallavicini A, Tretiach M. **2018**. Relation between water status and desiccation-affected genes in the lichen photobiont *Trebouxia gelatinosa*. *Plant Physiology and Biochemistry* **129**: 189–197.

Bao T, Zhu R, Li X, Ye W, Cheng X. **2018**. Effects of multiple environmental variables on tundra ecosystem respiration in maritime Antarctica. *Scientific Reports* **8**: 1–12.

Barták M, Váczi P, Hájek J, Smykla J. **2007**. Low-temperature limitation of primary photosynthetic processes in Antarctic lichens *Umbilicaria antarctica* and *Xanthoria*

elegans. *Polar Biology* **31**: 47–51.

Bjerke JW. **2011**. Winter climate change: Ice encapsulation at mild subfreezing temperatures kills freeze-tolerant lichens. *Environmental and Experimental Botany* **72**: 404–408.

Bokhorst S, Convey P, Huiskes A, Aerts R. **2016**. *Usnea antarctica*, an important Antarctic lichen, is vulnerable to aspects of regional environmental change. *Polar Biology* **39**: 511–521.

Candotto Carniel F, Zanelli D, Bertuzzi S, Tretiach M. **2015**. Desiccation tolerance and lichenization: a case study with the aeroterrestrial microalga *Trebouxia* sp. (Chlorophyta). *Planta* **242**: 493–505.

Centeno DC, Hell AF, Braga MR, del Campo EM, Casano LM. **2016**. Contrasting strategies used by lichen microalgae to cope with desiccation-rehydration stress revealed by metabolite profiling and cell wall analysis. *Environmental Microbiology* **18**: 1546–1560.

Colesie C, Büdel B, Hurry V, Green TGA. **2018**. Can Antarctic lichens acclimatize to changes in temperature? *Global Change Biology* **24**: 1123–1135.

Davey MC. **1989**. The effects of freezing and desiccation on photosynthesis and survival of terrestrial Antarctic algae and cyanobacteria. *Polar Biology* **10**: 29–36.

Demmig-Adams B, Iii WWA, Czygan F, Schreiber U, Lange OL. **1990**. Differences in the capacity for radiationless energy dissipation in the photochemical apparatus of green and blue-green algal lichens associated with differences in carotenoid composition. *Planta* **180**: 582–589.

Esteban R, Balaguer L, Manrique E, Rubio de Casas R, Ochoa R, Fleck I, Pintó-Marijuan M, Casals I, Morales D, Jiménez MS, *et al.* 2009. Alternative methods for sampling and preservation of photosynthetic pigments and tocopherols in plant material

from remote locations. *Photosynthesis Research* **101**: 77–88.

Esteban R, Barrutia O, Artetxe U, Fernández-Marín B, Hernández A, García-Plazaola JI. **2015**. Internal and external factors affecting photosynthetic pigment composition in plants: a meta-analytical approach. *New Phytologist* **206**: 268–280.

Fernández-Marín B, Atherton J, Olascoaga B, Kolari P, Porcar-Castell A, García-Plazaola JI. **2018a**. When the sun never sets: daily changes in pigment composition in three subarctic woody plants during the summer solstice. *Trees - Structure and Function* **32**: 615–630.

Fernández-Marín B, Becerril JM, García-Plazaola JI. **2010**. Unravelling the roles of desiccation-induced xanthophyll cycle activity in darkness: A case study in *Lobaria pulmonaria*. *Planta* **231**: 1335–1342.

Fernández-Marín B, Gago J, Flexas J, Gulías J. **2019**. Plant pigment cycles in the high-Arctic Spitsbergen. *Polar Biology* **42**: 675–684.

Fernández-Marín B, Kranner I, Sebastián MS, Artetxe U, Laza JM, Vilas JL, Pritchard HW, Nadajaran J, Míguez F, Becerril JM, *et al.* 2013. Evidence for the absence of enzymatic reactions in the glassy state. A case study of xanthophyll cycle pigments in the desiccation-tolerant moss *Syntrichia ruralis*. *Journal of Experimental Botany* **64**: 3033–3043.

Fernández-Marín B, Míguez F, Becerril JM, García-Plazaola JI. **2011a**. Dehydration-mediated activation of the xanthophyll cycle in darkness: Is it related to desiccation tolerance? *Planta* **234**: 579–588.

Fernández-Marín B, Míguez F, Becerril J, García-Plazaola J. **2011b**. Activation of violaxanthin cycle in darkness is a common response to different abiotic stresses: a case study in *Pelvetia canaliculata*. *BMC Plant Biology* **11**: 181.

Fernández-Marín B, Neuner G, Kuprian E, Laza JM, García-Plazaola JI,

Verhoeven A. **2018b**. First evidence of freezing tolerance in a resurrection plant: insights into molecular mobility and zeaxanthin synthesis in the dark. *Physiologia Plantarum* **163**: 472–489.

García-Plazaola JI, Becerril JM. **1999**. A rapid high-performance liquid chromatography method to measure lipophilic antioxidants in stressed plants: simultaneous determination of carotenoids and tocopherols. *Phytochemical Analysis* **10**: 307–313.

García-Plazaola JI, Becerril JM. **2001**. Seasonal changes in photosynthetic pigments and antioxidants in beech (*Fagus sylvatica*) in a Mediterranean climate: implications for tree decline diagnosis. *Australian Journal of Plant Physiology* **28**: 225–232.

Garrido-Benavent I, de los Ríos A, Fernández-Mendoza F, Pérez-Ortega S. **2018**. No need for stepping stones: Direct, joint dispersal of the lichen-forming fungus *Mastodia tessellata* (Ascomycota) and its photobiont explains their bipolar distribution. *Journal of Biogeography* **45**: 213–224.

Garrido-Benavent I, Pérez-Ortega S, de los Ríos A. **2017**. From Alaska to Antarctica: Species boundaries and genetic diversity of *Prasiola* (Trebouxiophyceae), a foliose chlorophyte associated with the bipolar lichen-forming fungus *Mastodia tessellata*. *Molecular Phylogenetics and Evolution* **107**: 117–131.

Gauslaa Y, Solhaug KA. **1999**. High-light damage in air-dry thalli of the old forest lichen Lobaria pulmonaria - Interactions of irradiance, exposure duration and high temperature. *Journal of Experimental Botany* **50**: 697–705.

Goudriaan J. **1982**. Potential production processes. In: Penning de Vries F, Van-Laar H, eds. Simulation of plant growth and crop production. Wageningen,: Pudoc:, 98–113.

Graham J, Wilcox L, Graham L. **2009**. *Algae*. San Francisco: Pearson Education.

Guéra A, Gasulla F, Barreno E. **2016**. Formation of photosystem II reaction centers

that work as energy sinks in lichen symbiotic Trebouxiophyceae microalgae. *Photosynthesis Research* **128**: 15–33.

Hájek J, Barták M, Hazdrová J, Forbelská M. **2016**. Sensitivity of photosynthetic processes to freezing temperature in extremophilic lichens evaluated by linear cooling and chlorophyll fluorescence. *Cryobiology* **73**: 329–334.

Harańczyk H, Grandjean J, Olech M, Michalik M. **2003**. Freezing of water bound in lichen thallus as observed by H NMR. II. Freezing protection mechanisms in a cosmopolitan lichen Cladonia mitis and in Antarctic lichen species at different hydration levels. *Colloids and Surfaces B: Biointerfaces* **28**: 251–260.

Hauck M, Jürgens SR, Brinkmann M, Herminghaus S. **2008**. Surface hydrophobicity causes SO_2 tolerance in lichens. *Annals of Botany* **101**: 531–539.

Heber U, Azarkovich M, Shuvalov V. **2007**. Activation of mechanisms of photoprotection by desiccation and by light: Poikilohydric photoautotrophs. *Journal of Experimental Botany* **58**: 2745–2759.

Heber U, Bilger W, Türk R, Lange OL. **2010**. Photoprotection of reaction centres in photosynthetic organisms: Mechanisms of thermal energy dissipation in desiccated thalli of the lichen *Lobaria pulmonaria*. *New Phytologist* **185**: 459–470.

Holzinger A, Herburger K, Blaas K, Lewis LA, Karsten U. **2017**. The terrestrial green macroalga *Prasiola calophylla* (Trebouxiophyceae, Chlorophyta): ecophysiological performance under water-limiting conditions. *Protoplasma* **254**: 1755–1767.

Holzinger A, Karsten U, Lütz C, Wiencke C. **2006**. Ultrastructure and photosynthesis in the supralittoral green macroalga *Prasiola crispa* from Spitsbergen (Norway) under UV exposure. *Phycologia* **45**: 168–177.

Huiskes A, Gremmen N, Francke J. **1997a**. The delicate stability of lichen symbiosis:

comparative studies on the photosynthesis of the lichen *Mastodia tesselata* and its free-living phycobiont, the alga *Prasiola crispa*. In: Battaglia B, Valencia J, Walton D, eds. Antarctic communities. Species, structures and survival. Yerseke, The Netherlands: Cambridge University Press, 234–240.

Huiskes A, Gremmen N, Francke J. **1997b**. Morphological effects on the water balance of Antarctic foliose and fruticose lichens. *Antarctic Science* **9**: 36–42.

Jackson AE, Seppelt RD. **1995**. The accumulation of proline in *Prasiola crispa* during winter in Antarctica. *Physiologia Plantarum* **94**: 25–30.

Jacob A, Kirst GO, Wiencke C, Lehmann H. **1991**. Physiological responses of the Antarctic green alga *Prasiola crispa* ssp. *antarctica* to salinity stress. *Journal of Plant Physiology* **139**: 57–62.

Jacob A, Kirst GO, Wiencke C, Lehmann H. **1992**. Physiology and ultrastructure of desiccation in the green alga *Prasiola crispa* from Antarctica. *Botanica Marina* **35**: 297–304.

Jassby AD, Platt T, Jassbyl AD. **1976**. Mathematical formulation of the relationship between photosynthesis and light for phytoplankton. *Limnology and Oceanography* **21**: 540–547.

Kang EJ, Scrosati RA, Garbary DJ. **2013**. Physiological ecology of photosynthesis in *Prasiola stipitata* (Trebouxiophyceae) from the Bay of Fundy, Canada. *Phycological Research* **61**: 208–216.

Kappen L. **1989**. Field measurements of carbon dioxide exchange of the Antarctic lichen *Usnea sphacelata* in the frozen state. *Antarctic Science* **1**: 31–34.

Kappen L. **2000**. Some aspects of the great success of lichens in Antarctica. *Antarctic Science* **12**: 314–324.

Kappen L, Lange OL. **1972**. Die Kälteresistenz einiger Makrolichenen. *Flora* **161**: 1–

29.

Kosugi M, Arita M, Shizuma R, Moriyama Y, Kashino Y, Koike H, Satoh K. **2009**. Responses to desiccation stress in lichens are different from those in their photobionts. *Plant and Cell Physiology* **50**: 879–888.

Kosugi M, Katashima Y, Aikawa S, Tanabe Y, Kudoh S, Kashino Y, Koike H, Satoh K. **2010**. Comparative study on the photosynthetic properties of *Prasiola* (chlorophyceae) and *Nostoc* (cyanophyceae) from antarctic and non-antarctic sites. *Journal of Phycology* **46**: 466–476.

Kosugi M, Maruo F, Inoue T, Kurosawa N, Kawamata A, Koike H, Kamei Y, Kudoh S, Imura S. **2018**. A comparative study of wavelength-dependent photoinactivation in photosystem II of drought-tolerant photosynthetic organisms in Antarctica and the potential risks of photoinhibition in the habitat. *Annals of Botany* **122**: 1263–1278.

Kosugi M, Miyake H, Yamakawa H, Shibata Y, Miyazawa A, Sugimura T, Satoh K, Itoh S, Kashino Y. **2013**. Arabitol provided by lichenous fungi enhances ability to dissipate excess light energy in a symbiotic green alga under desiccation. *Plant and Cell Physiology* **54**: 1316–1325.

Kosugi M, Shizuma R, Moriyama Y, Koike H, Fukunaga Y, Takeuchi A, Uesugi K, Suzuki Y, Imura S, Kudoh S, *et al.* 2014. Ideal osmotic spaces for chlorobionts or cyanobionts are differentially realized by lichenized fungi. *Plant Physiology* **166**: 337–348.

Kranner I. **2002**. Glutathione status correlates with different degrees of desiccation tolerance in three lichens. *New Phytologist* **154**: 451–460.

Kranner I, Beckett R, Hochman A, Nash TH. **2008**. Desiccation-tolerance in lichens: a review. *The Bryologist* **111**: 576–593.

Kranner I, Cram WJ, Zorn M, Wornik S, Yoshimura I, Stabentheiner E, Pfeifhofer HW. **2005**. Antioxidants and photoprotection in a lichen as compared with its isolated symbiotic partners. *Proceedings of the National Academy of Sciences* **102**: 3141–3146.

Kranner I, Zorn M, Turk B, Wornik S, Beckett RP, Batič F. **2003**. Biochemical traits of lichens differing in relative desiccation tolerance. *New Phytologist* **160**: 167–176.

Ladrón de Guevara M, Gozalo B, Raggio J, Lafuente A, Prieto M, Maestre FT. **2018**. Warming reduces the cover, richness and evenness of lichen-dominated biocrusts but promotes moss growth: Insights from an 8 yr experiment. *New Phytologist* **220**: 811–823.

Laguna-Defior C, Pintado A, Green TGA, Blanquer JM, Sancho LG. **2016**. Distributional and ecophysiological study on the Antarctic lichens species pair *Usnea antarctica/Usnea aurantiaco-atra*. *Polar Biology* **39**: 1183–1195.

Lizarazo K, Fernández-Marín B, Becerril JM, García-Plazaola JI. **2010**. Ageing and irradiance enhance vitamin E content in green edible tissues from crop plants. *Journal of the Science of Food and Agriculture* **90**: 1994–1999.

Lobo F de A, de Barros MP, Dalmagro HJ, Dalmolin ÂC, Pereira WE, de Souza ÉC, Vourlitis GL, Rodríguez Ortíz CE. **2013**. Fitting net photosynthetic light-response curves with Microsoft Excel - a critical look at the models. *Photosynthetica* **51**: 445–456.

López-Pozo M, J F, J G, M C, M N, AV P, MJ C, J G, E N, J M, *et al.* 2019. A field portable method for semi-quantitative estimation of dehydration tolerance of photosynthetic tissues across distantly related land plants. *Physiologia Plantarum*: doi:10.1111/ppl.12890.

Loriaux SD, Avenson TJ, Welles JM, Mcdermitt DK, Eckles RD, Riensche B, Genty B. **2013**. Closing in on maximum yield of chlorophyll fluorescence using a single multiphase flash of sub-saturating intensity. *Plant, Cell and Environment* **36**: 1755–1770.

Lud D, Huiskes A, Moerdijk T, Rozema J. **2001a**. The effects of altered levels of UV-B radiation on an Antarctic grass and lichen. *Plant Ecology* **154**: 89–99.

Lud D, Huiskes A, Ott S. **2001b**. Morphological evidence for the symbiotic character of *Turgidosculum complicatulum* Kohlm. & Kohlm. (= *Mastodia tesselata* Hook.f. & Harvey). *Symbiosis* **31**: 141–151.

Míguez F, Fernández-Marín B, Becerril JM, García-Plazaola JI. **2017**. Diversity of winter photoinhibitory responses: A case study in co-occurring lichens, mosses, herbs and woody plants from subalpine environments. *Physiologia Plantarum* **160**: 282–296.

Moniz MBJ, Rindi F, Novis PM, Broady PA, Guiry MD. **2012**. Molecular phylogeny of antarctic prasiola (prasiolales, trebouxiophyceae) reveals extensive cryptic diversity. *Journal of Phycology* **48**: 940–955.

Muggia L, Vancurova L, Škaloud P, Peksa O, Wedin M, Grube M. **2013**. The symbiotic playground of lichen thalli - a highly flexible photobiont association in rock-inhabiting lichens. *FEMS Microbiology Ecology* **85**: 313–323.

Nardini A, Marchetto A, Tretiach M. **2013**. Water relation parameters of six *Peltigera species* correlate with their habitat preferences. *Fungal Ecology* **6**: 397–407.

Nowak P, Harańczyk H, Kijak P, Marzec M, Fitas J, Lisowska M, Baran E, Olech MA. **2018**. Bound water behavior in *Cetraria aculeata* thalli during freezing. *Polar Biology* **41**: 865–876.

Ochyra R, Lewis Smith RI, Bednarek-Ochyra H. **2008**. *The illustrated moss flora of Antarctica.* (R Ochyra, R Lewis Smith, and H Bednarek-Ochyra, Eds.). Cambridge:

Cambridge University Press.

Øvstedal DO (Dag O, Lewis Smith RI (Ronald I. 2001. *Lichens of Antarctica and South Georgia*. Cambridge University Press.

Pavlova E, Kuzmin A, Pozdnyakov N, Maslov A. 2017. 15N – nitrate uptake and nitrogen exchange in the bionts of the lichen Parmelia sulcata. *Symbiosis* **72**: 117–121.

Peat HJ, Clarke A, Convey P. 2007. Diversity and biogeography of the Antarctic flora. *Journal of Biogeography* **34**: 132–146.

Pérez-Ortega S, de los Ríos A, Crespo A, Sancho LG. 2010. Symbiotic lifestyle and phylogenetic relationships of the bionts of *Mastodia tessellata* (Ascomycota, Incertae Sedis). *American Journal of Botany* **97**: 738–752.

Petruzzellis F, Savi T, Bertuzzi S, Montagner A, Tretiach M, Nardini A. 2018. Relationships between water status and photosystem functionality in a chlorolichen and its isolated photobiont. *Planta* **247**: 705–714.

Post A, Larkum AWD. 1993. UV-absorbing pigments, photosynthesis and UV exposure in Antarctica: comparison of terrestrial and marine algae. *Aquatic Botany* **45**: 231–243.

Proctor MCF, Nagy Z, Csintalan Z, Takács Z. 1998. Water-content components in bryophytes: Analysis of pressure-volume relationships. *Journal of Experimental Botany* **49**: 1845–1854.

Ritchie RJ, Prvan T. 1996a. A simulation study on designing experiments to measure the Km of Michaelis-Menten kinetics curves. *Journal of Theoretical Biology* **178**: 239–254.

Ritchie RJ, Prvan T. 1996b. Current statistical methods for estimating the Km and Vmax of Michaelis-Menten kinetics. *Biochemical Education* **24**: 196–206.

Sack L, Pasquet-Kok J, PrometheusWiki contributors. 2011. PrometheusWiki | Leaf

pressure-volume curve parameters. *PrometheusWiki*.

Sadowsky A, Ott S. **2012**. Photosynthetic symbionts in Antarctic terrestrial ecosystems: The physiological response of lichen photobionts to drought and cold. *Symbiosis* **58**: 81–90.

Sánchez FJ, Meeßen J, Ruiz M. del C, G.ª Sancho L, Ott S, Vílchez C, Horneck G, Sadowsky A, de la Torre R. **2014**. UV-C tolerance of symbiotic *Trebouxia* sp. in the space-tested lichen species *Rhizocarpon geographicum* and *Circinaria gyrosa*: role of the hydration state and cortex/screening substances. *International Journal of Astrobiology* **13**: 1–18.

Sancho LG, Pintado A, Navarro F, Ramos M, De MA, Blanquer JM, Raggio J, Valladares F, Allan TG. **2017**. Recent warming and cooling in the Antarctic Peninsula region has rapid and large effects on lichen vegetation. *Scientific Reports* **7**: 5689.

Sanders W, Moe R, Ascaso C. **2004**. The intertidal marine lichen formed by the Pyrenomycete fungus *Verrucaria tavaresiae* (Ascomycotina) and the brown alga *Petroderma maculiforme* (Phaeophyceae): thallus organization and symbiont interaction. *American Journal of Botany* **91**: 511–522.

Smith E. **1936**. Photosynthesis in relation to light and carbon dioxide. *Proceedings of the National Academy of Sciences of the United States of America* **22**: 504–511.

Smith VR, Gremmen N. **2001a**. *Turgidosculum complicatulum* on sub-Antarctic Marion Island: Carbon acquisition response to climate change. *Polar Biology* **24**: 455–459.

Smith VR, Gremmen NJM. **2001b**. Photosynthesis in a sub-Antarctic shore-zone lichen. *New Phytologist* **149**: 291–299.

Solhaug KA, Chowdhury DP, Gauslaa Y. **2018**. Short- and long-term freezing effects in a coastal (*Lobaria virens*) versus a widespread lichen (*L. pulmonaria*). *Cryobiology*

82: 124–129.

Solhaug KA, Larsson P, Gauslaa Y. **2010**. Light screening in lichen cortices can be quantified by chlorophyll fluorescence techniques for both reflecting and absorbing pigments. *Planta* **231**: 1003–1011.

Solhaug KA, Xie L, Gauslaa Y. **2014**. Unequal allocation of excitation energy between photosystem II and I reduces cyanolichen photosynthesis in blue light. *Plant and Cell Physiology* **55**: 1404–1414.

Strzalka K, Szymanska R, Suwalsky M. **2011**. Prenyllipids and pigments content in selected antarctic lichens and mosses. *Journal of the Chilean Chemical Society* **56**: 808–811.

Veerman J, Vasil'ev S, Paton GD, Ramanauskas J, Bruce D. **2007**. Photoprotection in the lichen *Parmelia sulcata*: The origins of desiccation-induced fluorescence quenching. *Plant Physiology* **145**: 997–1005.

Verhoeven AS, Adams WW, Demmig-Adams B. **1998**. Two forms of sustained xanthophyll cycle-dependent energy dissipation in overwintering *Euonymus kiautschovicus*. *Plant, Cell and Environment* **21**: 893–903.

Verhoeven A, García-Plazaola JI, Fernández-Marín B. **2018**. Shared mechanisms of photoprotection in photosynthetic organisms tolerant to desiccation or to low temperature. *Environmental and Experimental Botany* **154**: 66–79.

Legend to figures

FIG. 1 Collecting site: characterization and meteorology. (A) Collection field site: Argentina Cove in Livingston Island (Maritime Antarctica). (B) Detail of the microenvironment showing the intricate patched carpet formed by *M. tessellata* (blue arrows) and *P. crispa* (green arrows). (C) Gentoo penguin colony (red arrow) close to the studied populations**.** (D) Meteorological data for the summer of the study obtained from the BAE-JCI station: maximum and minimum day temperatures are depicted in red and black, respectively. Blue bars depict cumulative day precipitation. (E) Meteorological data for a month temporal window including the experimental days (23rd of February to 6th of March). Relative humidity (RH), average temperature and irradiance are presented as blue, orange lines, and grey lines, respectively. Vertical green lines highlight the measuring timepoints for YII (see Materials and Methods for further details).

FIG. 2. Boxplots showing the contents of photosynthetic pigment and tocopherol in *M. tessellata* and *P. crispa* thalli directly collected in the field. Boxes cover 50% of the data; central lines represent the medians and whiskers represent the minimum and maximum values among non-atypical data. Open circles represent outliers. The numbers of reported data are: (n=8) for *M. tessellata* and (n=9) for *P. crispa*. Asterisks denote significant differences ($p<0.05$) between both species analysed by one-way ANOVA. Units are mol to mol when no other unit is specified.

FIG. 3. Photochemical parameters measured in the field under natural irradiance (PPFD) for *M. tessellata* (dark green) and free-living *P. crispa* (light green). Upper panels show the response of actual photochemical efficiency of PSII (YII) to instantaneous irradiance over the thalli of (A) *M. tessellata* and (B) *P. crispa*. Data points are individual

measurements (n=122, per species). Lower panels show changes in the de-epoxidation index of xanthophyll cycle in response to last week cumulative irradiance (C) or precipitation (D). Data points are individual measurements (n=23 per species).

FIG. 4. Gas exchange data for *M. tessellata* (dark green) and *P. crispa* (light green) measured at +20 ºC in hydrated samples, in the lab of the BAE JCI. (A) Light curve of net CO_2 assimilation expressed on a thallus area basis. (B), (C), (D) and (E) depict: maximum net assimilation A_n (A_{sat}), dark respiration (R_d), irradiance at which 90% of A_{sat} is achieved (I_{sat90}) and light compensation point (I_{com}), respectively, calculated by Michaelis-Menten curve fitting. Data are mean values ± SE (n=4-5). Asterisks denote significantly different values ($p< 0.05$).

FIG. 5. (A, B) Pressure-volume (P-V) curves of thalli from *M. tessellata* and *P. crispa*, showing the changes of the inverse water potential ($1/\Psi$) as a function of water loss from the thalli (1-RWC). One representative measurement is shown for each species. (C-H) Selected parameters estimated from the P-V curves (see Materials and Methods for details on the calculations): water potential at full turgor (Ψo), water potential at the turgor loss point (Ψ_{TLP}), symplastic water content at full turgor (SWC), and modulus of elasticity (ε). Data are mean values ± SE (n=3, for *P. crispa*, 2 for *M. tessellata*). Asterisks denote significant differences among species at $p<0.05$.

FIG. 6. Physiological, biochemical and physicochemical responses of *M. tessellata* and *P. crispa* under controlled desiccation in darkness. (A) Final water content (WC) at the end of desiccation treatments under three different relative humidities (RH). (B) % of F_v/F_m recovery after desiccation and subsequent hydration. (C) De-epoxidation extent of

the xanthophyll cycle pigments (AZ/VAZ) at the end of controlled desiccation. Bars are average values ± SE (n=3). (D) Glass transition temperature (Tg) of samples equilibrated at 10% RH (n=3). (E) Recovery kinetic of F_v/F_m (in percentage) during rehydration of samples previously equilibrated to 50% RH. Data points are average ± SE (n=6). (F) Static contact angle of a 3 µL distilled water drop on thalli surface (n=10). When significant, differences between *P. crispa* and *M. tessellata* are depicted with an asterisk ($p<0.05$).

FIG. 7. Physiological and physicochemical parameters of hydrated thalli from *M. tessellata* and *P. crispa* subjected to controlled freezing. (A) Kinetics of F_v/F_m evolution during freezing (incubation at –20 ºC) and subsequent thaw at + 20 ºC. Data points are average ± SE (n=6). (B) De-epoxidation level of xanthophyll cycle before and after 48 h of incubation (n=3). (C) Freezing temperature ranges obtained from onset temperatures of exothermic peak recorded with differential scanning calorimetry during cooling scan (n=6; see Supplementary data Fig. S5 for representative examples of the scans). When significant, differences between *P. crispa* and *M. tessellata* are depicted with an asterisk ($p<0.05$).

Figure 1

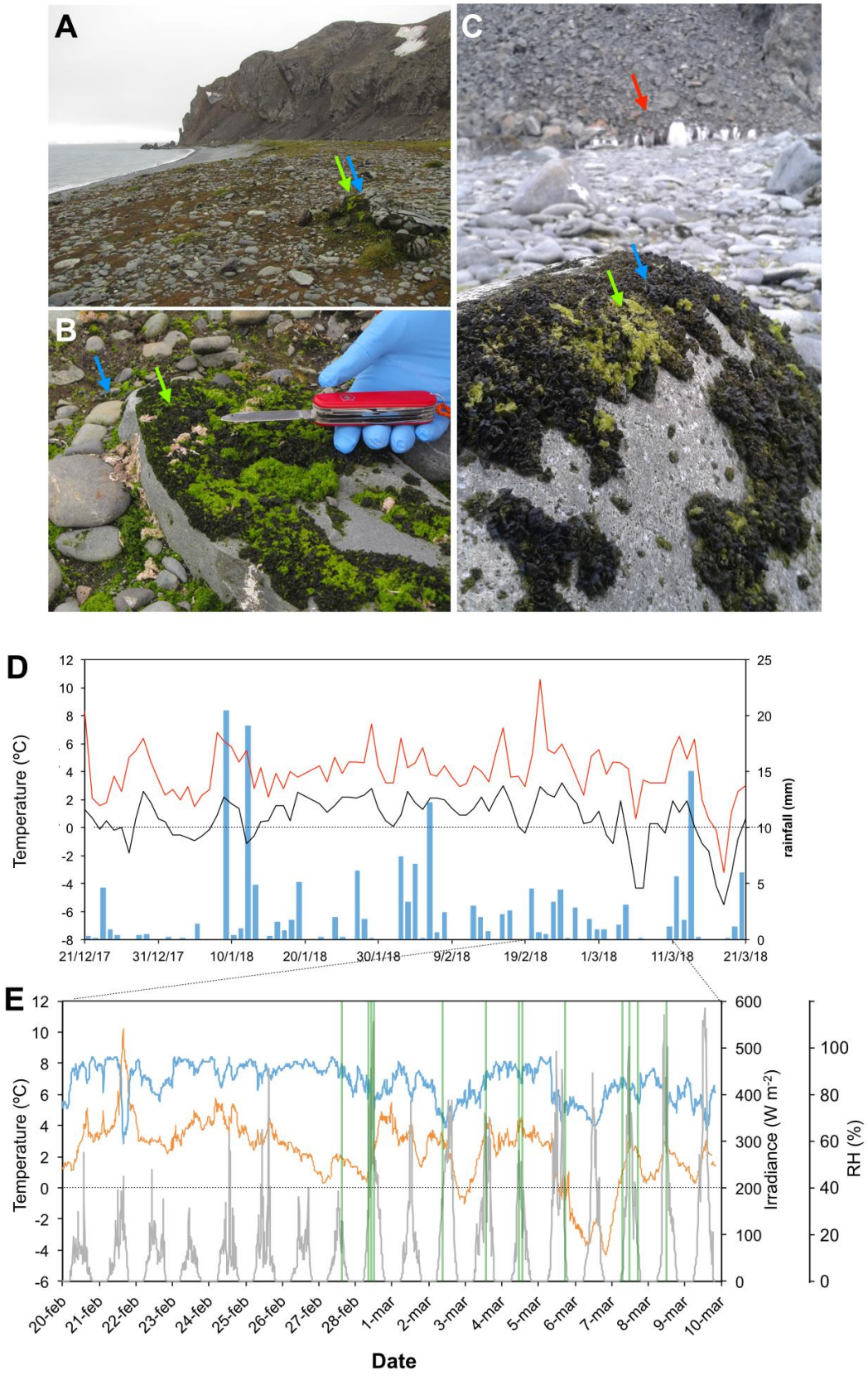

Figure 2

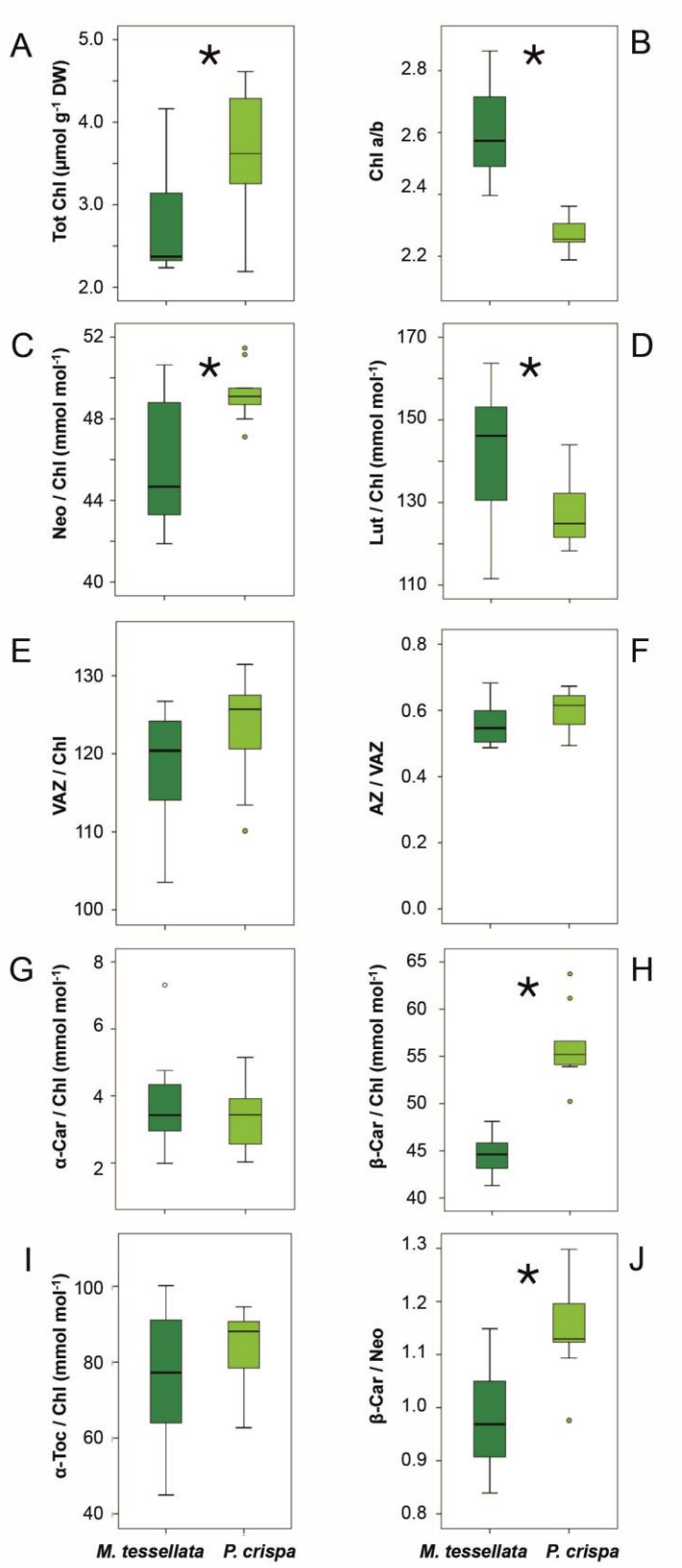

Figure 3

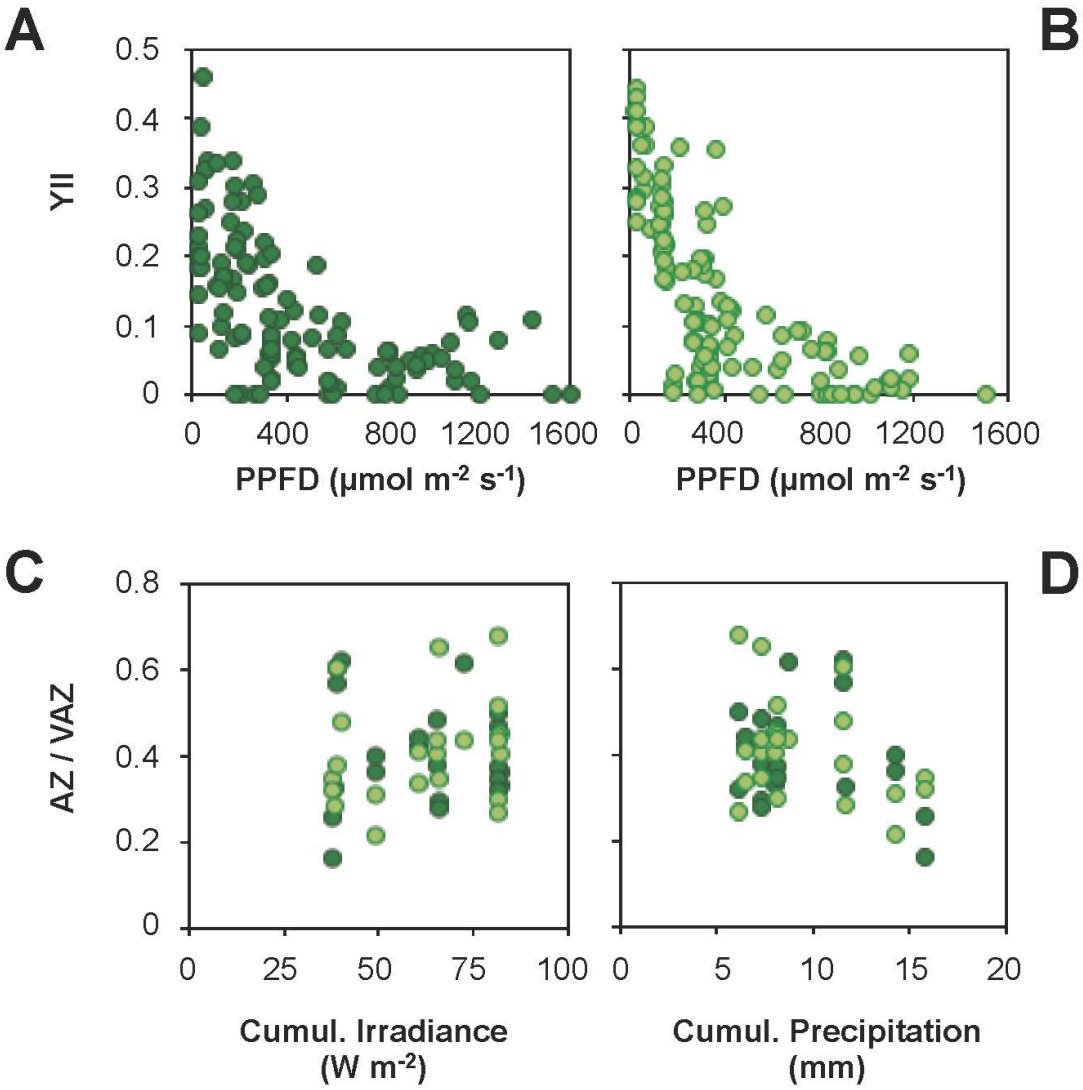

Figure 4

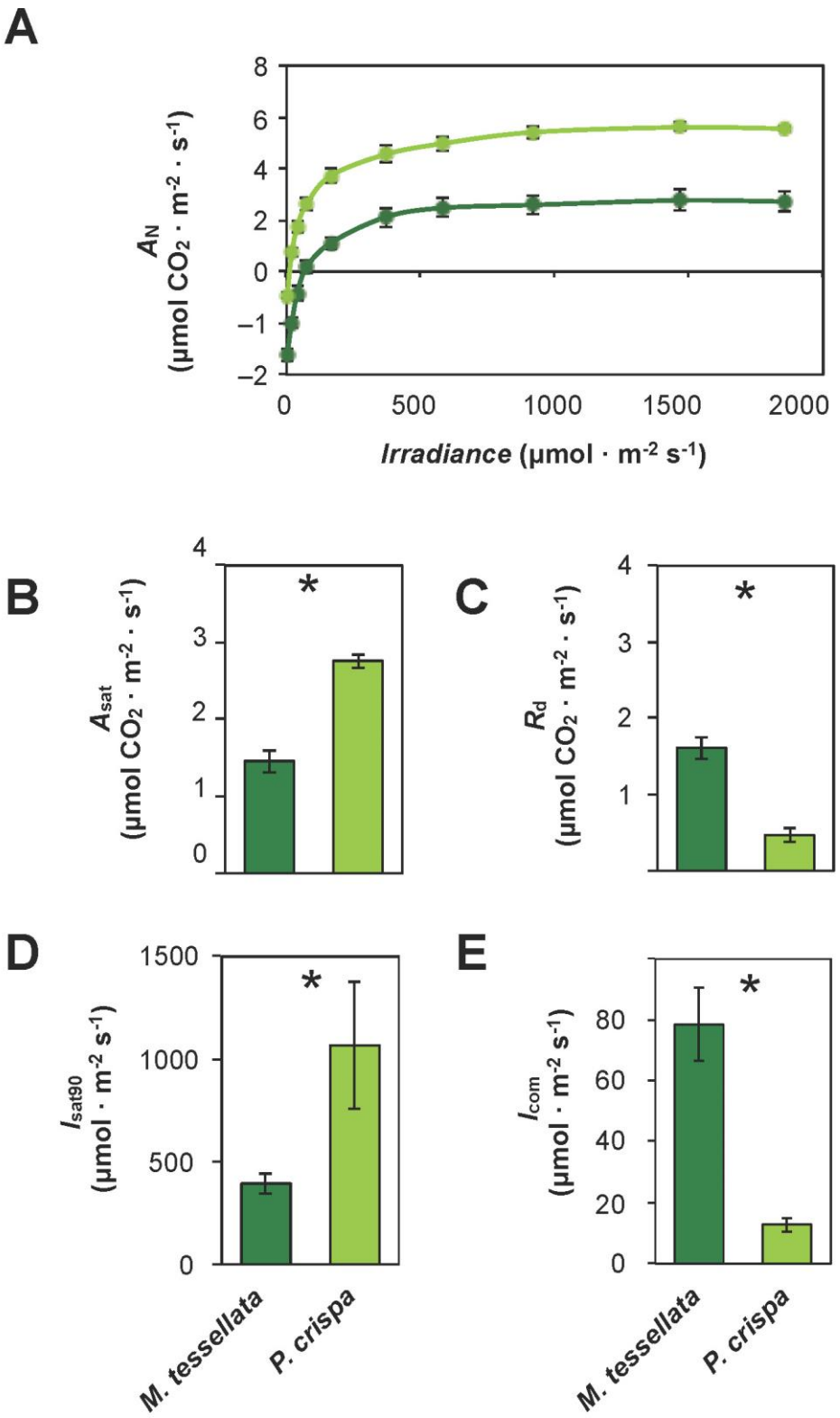

Figure 5

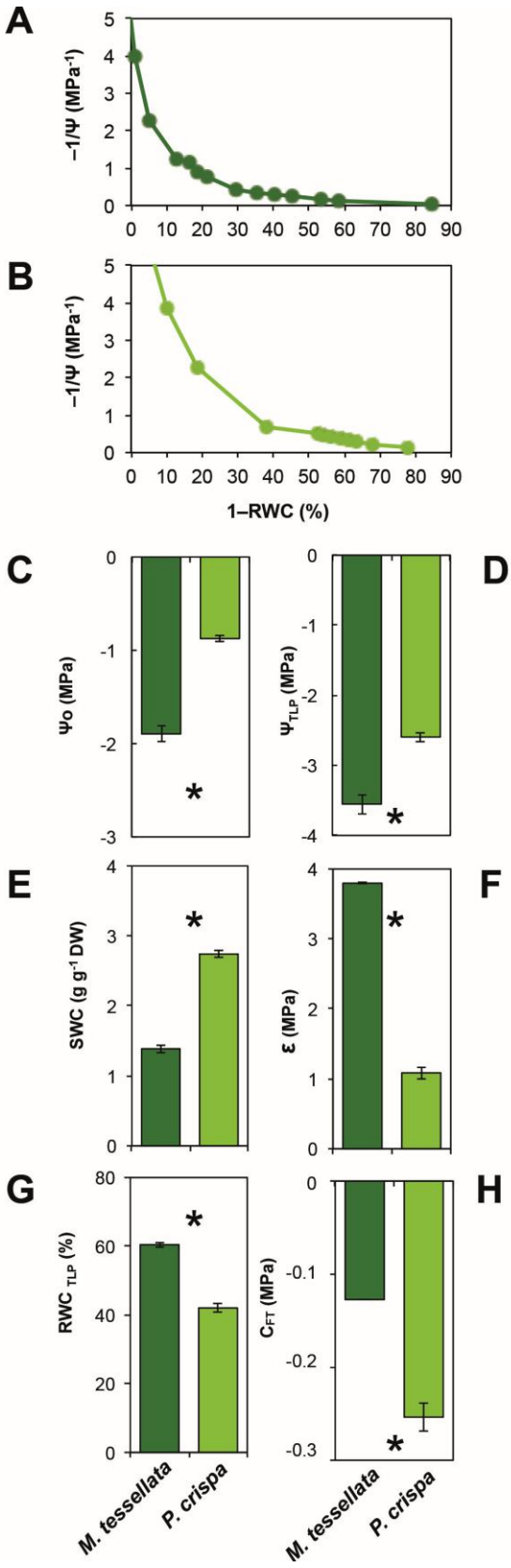

Figure 6

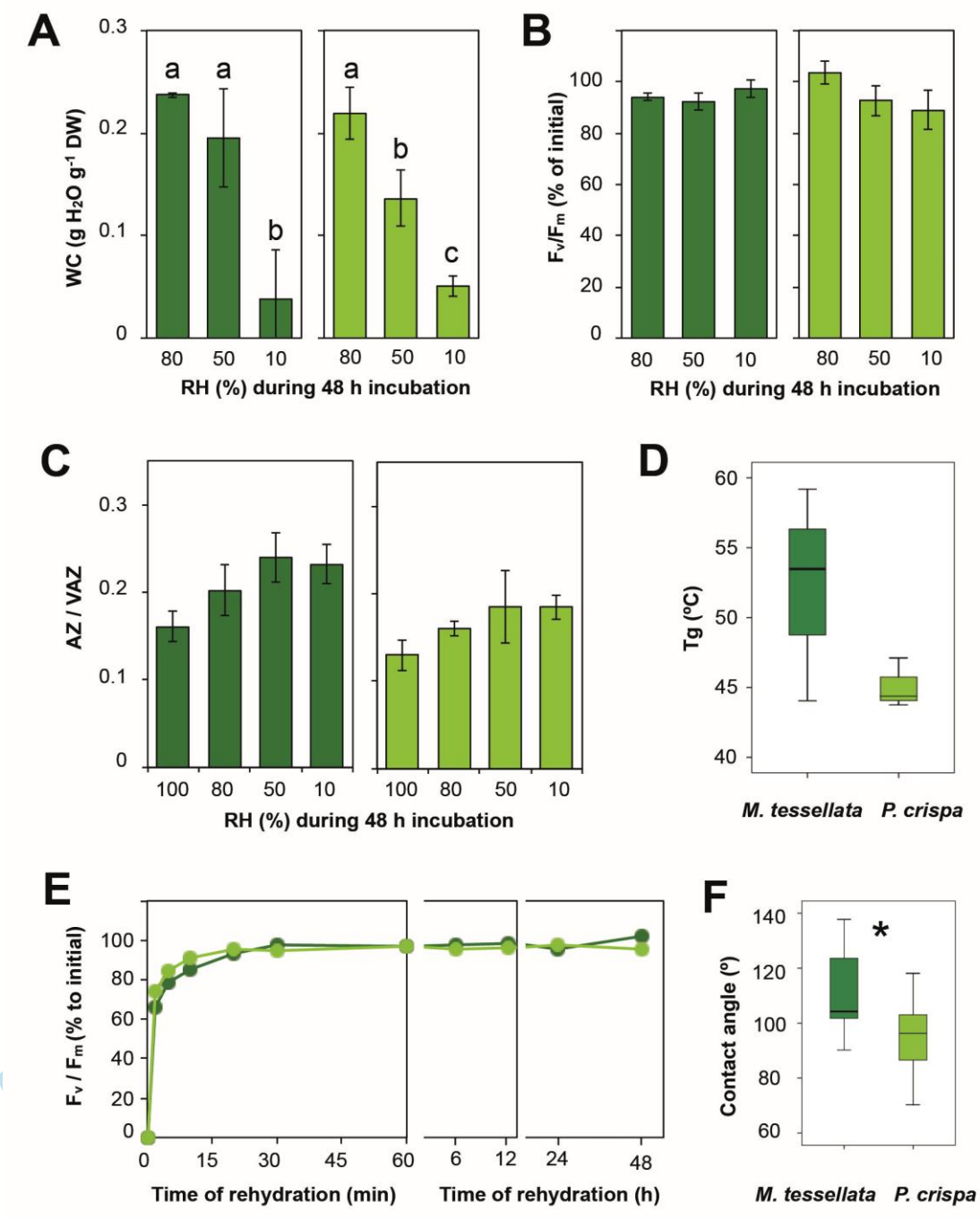

Figure 7